VOLUME 87 NO. ST2
FEBRUARY 1961

JOURNAL of the

Structural Division

PROCEEDINGS OF THE

AMERICAN SOCIETY OF CIVIL ENGINEERS

BASIC REQUIREMENTS FOR MANUSCRIPTS

Original papers and discussions of current papers should be submitted to the Manager of Technical Publications, ASCE. Authors should indicate the technical division to which the paper is referred. The final date on which a discussion should reach the Society is given as a footnote with each paper. Those who are planning to submit material will expedite the review and publication procedures by complying with the following basic requirements:

1. Titles must have a length not exceeding 50 characters and spaces.

2. A summary of approximately 50 words must accompany the paper, a 300-word synopsis must precede it, and a set of conclusions must end it.

3. The manuscript (an original ribbon copy and two duplicate copies) should be double-spaced on one side of 8½-inch by 11-inch paper. Three copies of all illustrations, tables, etc., must be included.

4. The author's full name, Society membership grade, and footnote reference stating present employment must appear on the first page of the paper.

5. Mathematics are recomposed from the copy that is submitted. Because of this, it is necessary that letters be drawn carefully, and that special symbols be properly identified. The letter symbols used should be defined where they first appear, in the illustrations or in the text, and arranged alphabetically in an Appendix.

6. Tables should be typed (an original ribbon copy and two duplicate copies) on one side of 8½-inch by 11-inch paper. Specific illustrations and explanation must be made in the text for each table.

7. Illustrations must be drawn in black ink on one side of 8½-inch by 11-inch paper. Because illustrations will be reproduced with a width of between 3-inches and 4½-inches, the lettering must be large enough to be legible at this width. Photographs should be submitted as glossy prints. Explanations and descriptions must be made within the text for each illustration.

8. The desirable average length of a paper is about 12,000 words and the absolute maximum is 18,000 words. As an approximation, each full page of typed text, table, or illustration is the equivalent of 300 words.

9. Technical papers intended for publication must be written in the third person.

10. The author should distinguish between a list of "Reading References" and a "Bibliography," which would encompass the subject of his paper.

This Journal is published monthly by the American Society of Civil Engineers. Publication office is at 2500 South State Street, Ann Arbor, Michigan. Editorial and General Offices are at 33 West 39 Street, New York 18, New York. $4.00 of a member's dues are applied as a subscription to this Journal. Second-class postage paid at Ann Arbor, Michigan.

The index for 1959 was published as ASCE Publication 1960-10 (list price $2.00); indexes for previous years are also available.

Journal of the

STRUCTURAL DIVISION

Proceedings of the American Society of Civil Engineers

CONTENTS

February, 1961

Papers

DISCUSSION

(over)

Journal of the
STRUCTURAL DIVISION
Proceedings of the American Society of Civil Engineers

TESTS OF COMPOSITE BEAMS WITH STUD SHEAR CONNECTORS

By Charles Culver,[1] A.M. ASCE, and Robert Coston,[2] A.M. ASCE

SYNOPSIS

Composite concrete-steel beams using L shaped stud shear connectors were tested. Both static and fatigue tests were conducted. These tests indicate that present design specifications are extremely conservative.

INTRODUCTION

Composite beams, beams in which a concrete slab and steel beam act as an integral unit, are widely used in bridge and building construction. The essential element of the composite section is the shear connection between the slab and steel beam. The function of this connection is to resist the horizontal shear between the slab and beam and to prevent uplift of the slab from the steel beam.

A variety of devices, including channels, Zee sections, and spirals have been used as shear connectors. Economic considerations have lead to the development and use of round studs in place of the prior mentioned connectors. Simplicity and ease of installation make these studs advantageous.

The design of stud and other shear devices is based on an elastic analysis of the composite section and, for highway bridges, is governed by the AASHO specification.[3]

Note.—Discussion open until July 1, 1961. To extend the closing date one month, a written request must be filed with the Executive Secretary, ASCE. This paper is part of the copyrighted Journal of the Structural Division, Proceedings of the American Society of Civil Engineers, Vol. 87, No. ST 1, February, 1961.

[1] Research Asst., Fritz Engrg. Lab., Lehigh Univ., Bethlehem, Pa.

[2] Engrg. Trainee, Genl. Foods Corp., Jacksonville, Fla.

[3] "Standard Specifications for Highway Bridges," Amer. Assn. of Highway Officials, Sect. 9, Washington, D. C., 1957, p. 105.

This specification lists formulas for determining the "useful capacity" of shear connectors or the maximum load which a shear connector can carry and satisfactorily perform its function.

The criterion used in establishing values for the "useful capacity" of a shear connector was a limiting value of residual slip or horizontal displacement between the slab and steel beam after unloading of the composite section. The value of this residual slip was set[4] at 0.003 in. and it was stated that slip beyond this value, "causes an appreciable increase of both the stresses and deflections of the T-beam."[5]

This value of 0.003 in. is considerably below the slip at failure obtained from pushout tests of various types of connectors. Hence, the "useful capacity" is considerably below the ultimate connector strength. The resulting emergency reserve strength[6] (ultimate connector force/"useful capacity" force) for the studs is therefore greater than the emergency reserve strength (ultimate moment/yield moment) for the composite section. If increased slip did not alter the performance of the composite beam, then it seems feasible that larger values for the "useful capacity" of the connector could be used.

The objectives of this investigation were to determine:

1. The value of connector forces for studs such that the composite section will develop the ultimate moment.
2. The influence of slip on the load-deflection characteristics of a composite beam.
3. The effect of fatigue loading on a composite section.

Notation.—The letter symbols adopted for use in this paper are defined and arranged alphabetically, for convenience of reference, in Appendix II (Fig. 1).

DESIGN AND FABRICATION OF TEST SPECIMENS

Three specimens to be statically loaded and a fatigue specimen were designed for this series of tests. The design procedure used considers equilibrium of the concrete slab as a free body between sections of zero moment and ultimate moment and is based on the assumption that the shear connectors possess sufficient ductility so that a redistribution of the horizontal shearing forces is possible. This same assumption is used in the design of a riveted connection. Analysis of a previous test established the validity of this assumption.[7]

The shear connectors for the static tests were designed so that the connector forces at ultimate moment would be 1.6, 2.4 and 3.0 times the "useful capacity" according to the AASHO specification. The fatigue specimen was designed so that the shear stress, computed on the basis of a uniform distribution of shear

---

[4] "Investigation of Stud Shear Connectors for Composite Concrete and Steel I-Beams," by I. M. Viest, Journal, ACI, Vol. 27, No. 8, April, 1956, p. 875.

[5] "Development of the New AASHO Specifications for Composite Steel and Concrete Bridges," by I. M. Viest, R. S. Fountain and C. P. Siess, Bulletin No. 174, Highway Research Bd., 1958.

[6] "Advanced Mechanics of Materials," by F. B. Seely and J. O. Smith, John Wiley and Sons, New York, N. Y., 1955.

[7] "Composite Beams with Stud Shear Connectors," by Bruno Thürlimann, Highway Research Bd., Natl. Academy of Science, Bulletin 174, 1958, p. 18.

stress on the cross section of the stud, would approach the fatigue strength, based on a fatigue life of 2×10^6 cycles, obtained in previous pushout tests.[8] Design computations are included in Appendix I.

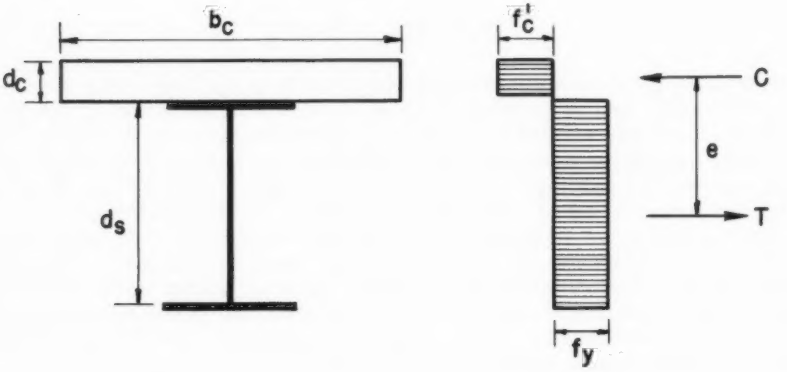

FIG. 1.—NOTATION

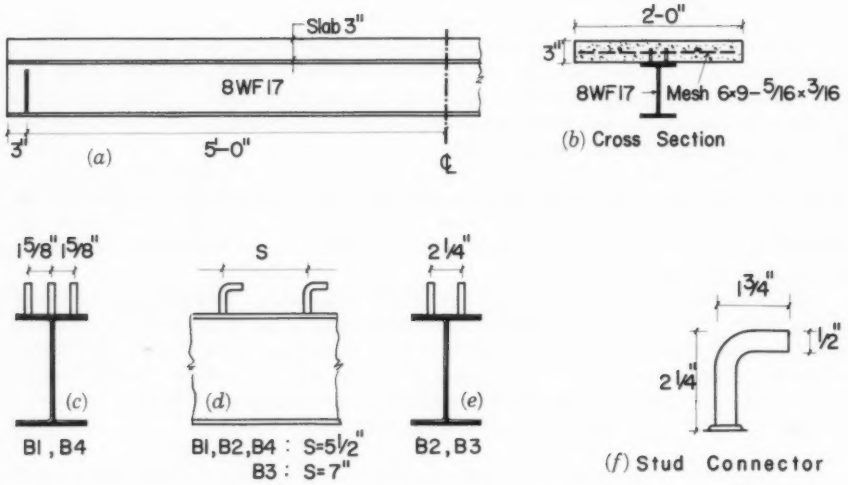

FIG. 2.—DIMENSIONS OF TEST SPECIMENS

Each of the four specimens consisted of a flat concrete flab connected to an 8WF17 beam by 1/2 in. diam. L shaped studs. Slab reinforcement consisted of

8 "Fatigue and Static Strength of Stud Shear Connectors," by Bruno Thürlimann, Journal, ACI, Vol. 30, June, 1959.

a mesh of 5/16 in. and 3/16 in. diam. rods. Fig. 2 gives the specimen dimensions and the connector spacings.

Forming and pouring of the specimens was done at Fritz Engineering Laboratory, Lehigh Univ. All beams were poured at the same time using a commercial ready mix concrete with a maximum aggregate size of 3/4 in.

TEST PROCEDURE

The specimens were simply supported over a span of 10ft and loaded with two point loads spaced symmetrically with respect to the center of the beam (Fig. 3). Load was applied by means of a hydraulic jack. In the static tests, an Amsler pendulum dynamometer applied and measured the pressure in the jack. An Amsler pulsator was connected to the jack to produce the cyclic, sinusolidally varying load at 250 cycles per min for the fatigue test.

The ultimate load at which crushing of the concrete slab will occur can be determined quite accurately. By stopping the tests short of this load, the loading positions can be changed to produce greater shearing forces for the same ultimate moment, in other words, increasing the spread "b" of the two concentrated loads (Fig. 4 and Table 1). Thus a single specimen can be used for several ultimate load tests and connector failure insured.

The prior mentioned procedure was followed in this series of tests with the load spacings designated as follows:

Spacing 1 (Test 1) — 2 b = 24 in.
Spacing 2 (Test 2) — 2 b = 36 in.
Spacing 3 (Test 3) — 2 b = 46 in.

Since all the specimens were similarly constructed, the only exception being the spacing and number of shear connectors, the value of M_p and hence P_p, for any given load spacing, should be the same for all specimens. Thus, the three static test beams are grouped according to the load spacing in Table 2, so that certain comparisons can be made later.

In the static tests, load was applied in increments of 5 kips up to the yield load. After exceeding the yield load a deflection criterion was used to determine the load increments. These increments were chosen so that the increase in deflection produced by each load increment was equal to the measured deflection of the specimen at the yield load.

Strain measurements in the slab and steel beam, center line and quarter point deflections, and end slip readings were recorded after each load increment. After reaching the yield load of the steel beam, the load was released periodically and residual deflection and end slip readings were recorded. The arrangement of the recording gages and the test setup are shown in Fig. 3.

The fatigue test of specimen B4 was conducted as follows:

1. 1,000,000 load cycles alternating between a minimum of 3,000 and a maximum of 30,000 lb.
2. 500,000 cycles between 3,000 and 36,000 lb.
3. 500,000 cycles between 3,000 and 42,000 lb.
4. Cyclic loading between 3,000 and 48,000 lb to failure of the specimen.

The load spacing was kept constant at 2 b = 36 in. Maximum slip and deflection under the fatigue loading were recorded by special gages. The fatigue loading

was stopped periodically and a load equal to the maximum cyclic load for that phase of the test was applied statically. Deflection, end slip, and strain readings

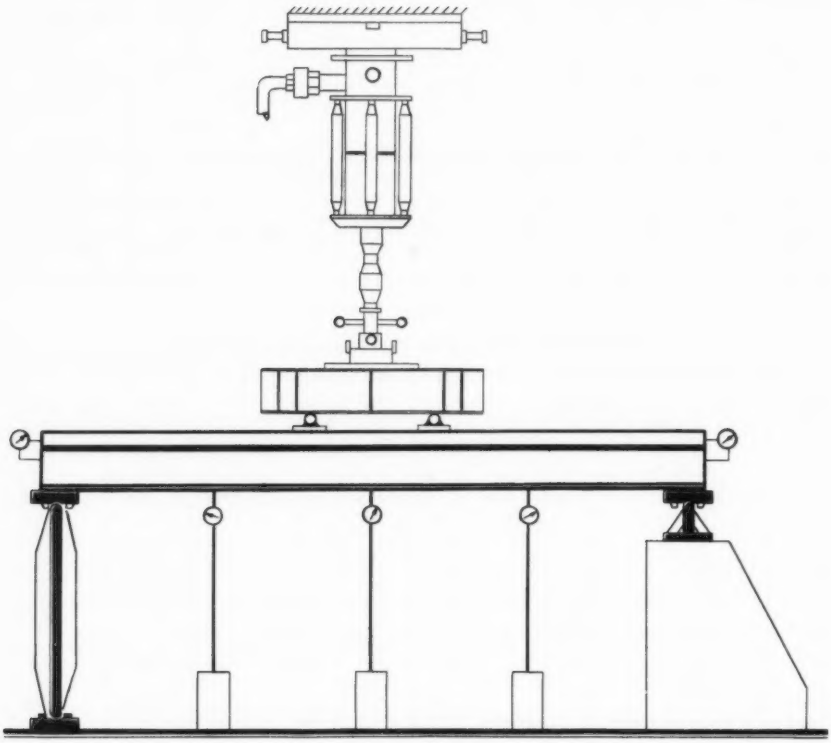

FIG. 3.—TEST SETUP

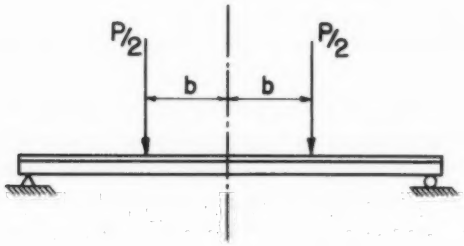

FIG. 4.—DESIGNATION OF SPECIMENS

were taken at this static load to determine the effect which the fatigue loading produced on the specimen.

TABLE 1.—DESIGNATION OF SPECIMENS

Specimen (1)	Stud spacing c, in in. (2)	Test No. (3)	Load spacing 2 b, in in. (4)	Loading (5)	Test Designation (6)
B1	3 at 5.5 in.	1	24	Static	B1-T1
B2	2 at 5.5 in.	1	24	Static	B2-T1
		2	36		B2-T2
B3	2 at 7.0 in.	1	24	Static	B3-T1
		2	36		B3-T2
		3	46		B3-T3
B4	3 at 5.5 in.	1	36	Fatigue	B4-T2

TABLE 2.—SUMMARY OF STATIC TEST RESULTS

Specimen (1)	Test (2)	Load spacing 2 b, in in. (3)	Failure type[a] (4)	Load P, in kips		C_L Moment M, in kips in.		Connector force,[b] Q, in kips (9)	Maximum end slip at P_u, in in. (10)	Residual end slip, in in. (11)
				P_p (5)	P_u (6)	M_p (7)	M_u (8)			
B 1	B1-T1	24	(A)	48.5	48.5	1165	1164	7.0	0.0044	0.0028
B 2	B2-T1		(B)		48.0		1150	10.6	.0089	.0060
B 3	B3-T1		(B)		47.5		1140	13.4	.0218	.0165
B 2	B2-T2	36	(A)	55.5	55.0		1155	12.1	.0446[c]	.0453
B 3	B3-T2		(B)		54.0		1132	15.4	.0712[c]	.0639
B 3	B3-T3	46	(C)	63.0	58.0		1071	16.1	.0925[c]	. . .

[a] Failure Type: (A) Bending failure by crushing of slab; (B) Test stopped short of crushing of slab; and (C) Shearing of studs.
[b] Connector force Q computed for the load P_u
[c] Residual end slip from previous test included

TABLE 3.—STATIC YIELD LEVEL OF MATERIAL IN 8WF17

Coupon No. (1)	Material (2)	Location of coupon (3)	Static yield stress, in ksi (4)
1	ASTM A-7 Structural Steel	Flange	36.0
2			38.1
3			36.8
4			36.7
		Average	36.9

Auxiliary tests included concrete cylinder tests and tensile coupon tests to determine the material properties of the composite section. The tensile coupons were taken from the unyielded portion of the flange of the steel beam after completion of testing. The results of these auxiliary tests appear in Tables 3 and 4.

RESULTS AND INTERPRETATION

Static Tests.—The results of the static tests are summarized in Table 2. The accuracy with which the ultimate load can be determined, assuming adequate shear connection, is shown by comparison of P_p and P_u for those tests in which bending failure occurred (failure type (A)). Values of P_u obtained for tests designated by failure type (B) are smaller than P_p because the tests were purposely

TABLE 4.—CYLINDER STRENGTH OF CONCRETE IN SLAB

Cylinder No. (1)	Age at test, in days (2)	Strength, in psi (3)
B-1	28	5800
B-2-A	28	5480
B-3-A	28	5390
	Average	5556
B-2-B	35	5670
B-3-B	35	5540
	Average	5605
B-3-C	42	5720
B-4-A	42	5390
B-4-B	42	5480
	Average	5530
	Cumulative Average	5563

stopped short of crushing of the slab and, strictly speaking, they are not really ultimate loads. In test B3-T3 the connectors failed before P_p was reached.

The average connector forces, computed by the same procedure used in the specimen design, are listed in Table 2. For those tests in which the ultimate moment was not reached, that is, when the test was stopped short of crushing of the concrete or the connectors failed, the connector forces were computed by multiplying the computed values for connector forces at ultimate ("Computation of Shear Flow" in Appendix I) by the ratio of the moment reached to the ultimate moment. All the values listed are greater than the "useful capacity" of the studs according to the AASHO specification. The values for residual end slip are also considerably larger than the value of 0.003.

Fig. 5 shows the load-slip curves for the three specimens. The load per connector in Beam 1 was close to the "useful capacity" load according to AASHO, whereas the maximum load per connector obtained in Beam 3, Test 3, was ap-

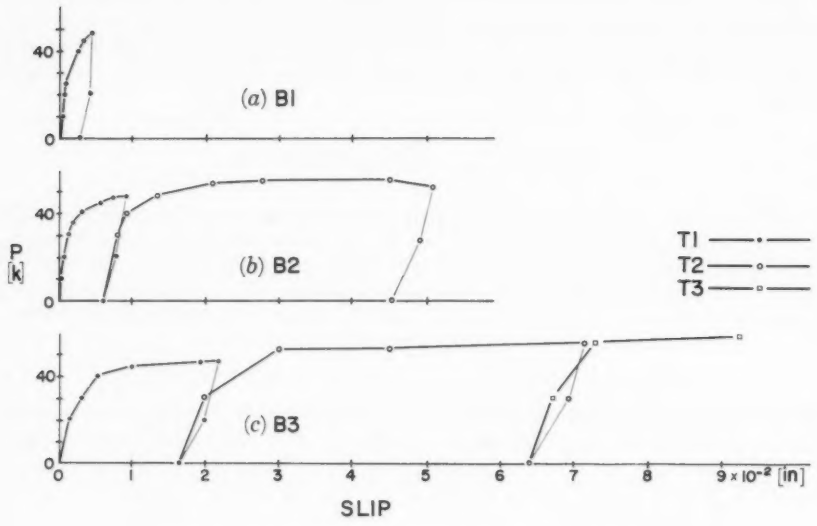

FIG. 5.—LOAD-SLIP CURVES FOR STATIC TESTS

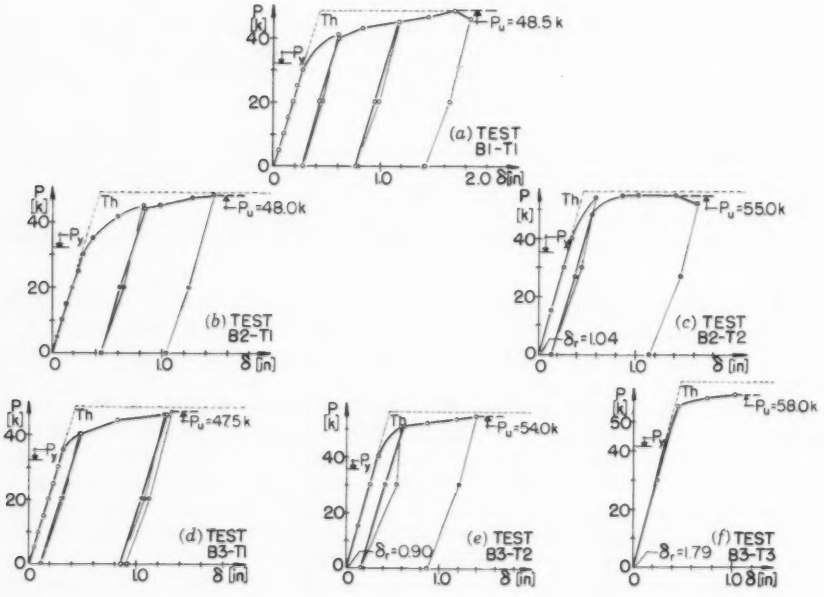

FIG. 6.—LOAD DEFLECTION CURVES FOR STATIC TESTS

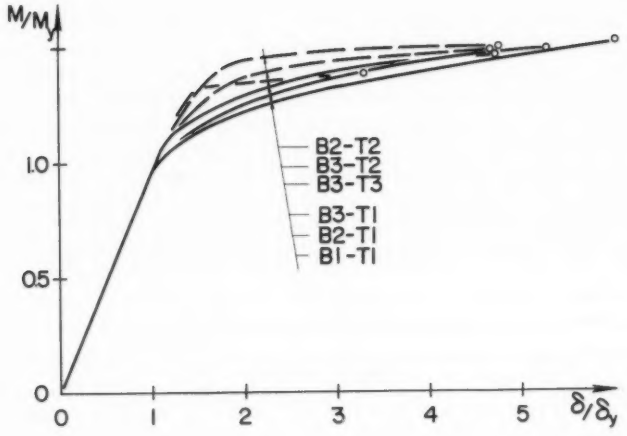

FIG. 7.—COMPARISON OF STATIC TESTS

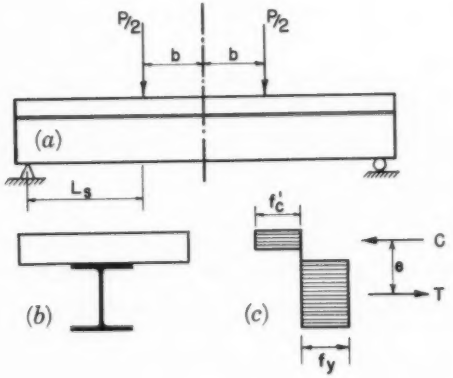

FIG. 8

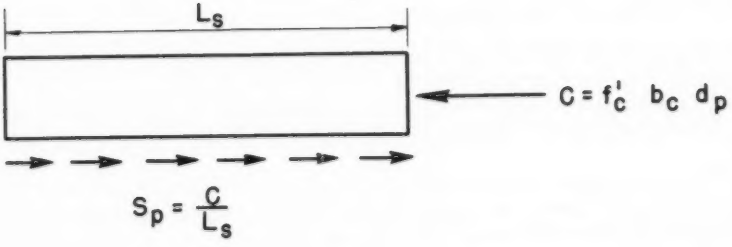

FIG. 9

proximately 2.5 times the "useful capacity." It is significant to note the large differences in slip which resulted from this increased connector loading.

Load deflection curves (shearing deflections included) for the various tests are presented in Fig. 6. Each test is plotted separately with its residual deflection from a previous test indicated at the origin. In order to compare the load deflection characteristics for all the tests, the non-dimensional graph of Fig. 7 was plotted. Despite the fact that there was a wide variation in connector forces between the various tests, this plot shows that the effect on the load deflection characteristics was relatively small. Up to yielding of the steel beam the behavior of all the specimens was exactly the same. Beyond this point there is a small difference between the various specimens. However, it is significant to note that all the curves tend to parallel the curve for B1-T1 and would have reached the same point at ultimate had they not been stopped short of crushing

TABLE 5.—FATIGUE TEST RESULTS

Load Range, in kips		Number of cycles	Total cycles	Deflection			Maximum Shear Stress in stud,[a] in ksi	End slip at P_{max} applied statically, in in. x 10-4
				Maximum during cyclic loading, in in.	At P_{max} applied statically, in in.	Theoretical, in in.		
P_{min}	P_{max}							
(1)	(2)	(3)	(4)	(5)	(6)	(7)	(8)	(9)
3	30	249,800	249,800	. . .	0.219	0.237	15.0	11
3	30	253,000	502,800	0.262	0.218	0.237	15.0	13
3	30	520,100	1,022,900	0.272	0.223	0.237	15.0	17
3	36	250,900	1,273,800	0.309	0.267	0.284	18.1	22
3	36	254,500	1,528,300	0.311	0.266	0.284	18.1	22
3	42	619,900	2,148,200	0.388	0.328	0.332	21.2	33
3	48	122,400	2,270,600	. . .	. . .	. . .	24.1	37

[a] Computed on the basis of a uniform distribution of shear stress on the cross section of the stud.

of the concrete. Only in B3-T3 in which the connector force reached 16 kips was there a reduction of M/M_y. It is evident that connector forces considerably in excess of the present AASHO "useful capacity" do not alter the performance of the composite section.

In summary, the following is to be noted:

1. The ultimate strength of stud connectors is considerably above the "useful capacity" according to AASHO.
2. Large values of slip between slab and beam do not significantly alter the ultimate moment or the load deflection characteristics of the composite section.
3. The emergency reserve strength of the studs (ultimate connector force/"useful capacity" force) is considerably larger than the emergency reserve strength of the beam (ultimate moment/yield moment).

Fatigue Test.—The fatigue test results are presented in Table 5. Note that there is a good correlation between the theoretical deflections and those obtained during testing. Computations indicated that the dynamic effects of loading were negligible. The increase in deflection under cyclic loading over both the theoretical deflection and the deflection under static loading could possibly be due to overloading by the jack.

The fatigue strength of the studs in this beam test is larger than values obtained in fatigue tests of connectors in pushout specimens.[8] This would indicate that there are certain factors which must be evaluated before a comparison between beam tests and pushout tests can be made. Frictional forces developed under the loading points in a beam test is one such factor. A comparison of beam tests and pushout tests does, however, seem feasible. Such a comparison would be advantageous because relatively small specimens (pushout specimens) could then be used to determine the strength of shear connectors. These additional factors probably account for the increase in connector forces also observed in the static tests over connector forces observed in static pushout tests.[8]

CONCLUSIONS

This series of tests has indicated that present specifications do not take into account the maximum useful strength on a static or fatigue basis of stud shear connectors. Further, it has been shown that loading these studs to ultimate does not alter the behavior of the composite section.

A design procedure for composite beams which would take into account the full strength of the elements of the composite section, that is, plastic design, seems feasible. There are, however, many questions which must be answered before such a design code can be formulated. Further research is required to answer such questions as:

1. Distribution and spacing of shear devices along the beam.
2. Interaction created by bond and friction.

Even if an elastic analysis is adhered to, these tests have shown that it is possible to increase the so called "useful capacity" shear connector force.

ACKNOWLEDGMENTS

This report was prepared as a term paper in partial fulfillment of the requirements for an undergraduate course in Civil Engineering at Lehigh Univ. The work was done under the supervision of Bruno Thurlimann, M. ASCE.

The authors wish to express their appreciation to Maurice E. Bender, F. ASCE, of Knoerle, Graef, Bender, and Associates, Inc. for financial support for the tests, and to KSM Products, Inc., Merchantville, N.J. for contributing the steel beams and shear connectors.

The testing was carried out at the Fritz Engineering Laboratory, Lehigh Univ., Bethleham, Pa. William J. Eney, F. ASCE, is Director of the Laboratory and Head of the Department of Civil Engineering.

APPENDIX I.—NOTATION

Section Properties

1. Concrete slab
   - b_c = 24 in.
   - d_c = 3 in.
   - f'_c = 5500 psi

2. Steel beam (8 WF 17)
   A_s = 5.00 sq in.
   d_s = 8.00 in.
   I_s = 56.0 $in.^4$
   f_y = 37.0 ksi

3. Studs
   diameter = 1/2 in.
   height = 2.25 in.
   area = 0 = 0.196 sq in.

4. Composite section
   ast = 7.25 in.
   I = 151.3 $in.^4$
   m (inner face of slab) = 16.2 $in.^3$
   n = 10

In the design of the test specimens, values for f'_c and f_y were assumed to be 3 ksi and 38 ksi, respectively. The cylinder tests and coupon tests gave average values of f'_c = 5563 psi and f_y = 36.9 Kips per sq in. The design computations were then revised using rounded off values of f'_c = 5500 psi and f_y = 37 Kips per sq in. and only these revised computations appear here.

AASHO Design.—Section 9 of the AASHO specification outlines the procedure to be used in the design of composite beams.

The three static test specimens considered in this paper were designed on an ultimate basis. Therefore, a direct comparison with the AASHO specification cannot be made since the latter follows an elastic analysis of the composite section. An estimate of the emergency reserve strength and the true factor of safety or "load factor" can be achieved by a comparison of the test results and values obtained from an analysis according to the AASHO specification.

For this purpose, a design of the shear connectors according to the AASHO specification follows:

1. Conventional design (allowable stress in bottom flange 18 Kips per sq in.).
   (a) Studs

$$\frac{H}{d} \geq 4.2$$

$$Q_{uc} = 330\, d^2 \sqrt{f'_c}$$
$$= 330\,(0.5)^2 \sqrt{5500} = 6110 \text{ lb}$$

   (b) Factor of safety

$$F.S. = \frac{2.7\left(1 + C_{mc} + C_{mi}\, C_s\right) - \left(C_{mc} + C_{mi}\right) + C_v}{\left(1 + C_v\right)}$$

$$C_s = \frac{\frac{151.3}{7.5}}{\frac{56.4}{4}} = 1.48$$

$$C_v = \frac{0.46 \text{ kips}}{20 \text{ kips}} = 0.023 \cong 0$$

$$C_{mc} = \frac{24.8 \text{ kip in.}}{1080 \text{ kip in.}} = 0.023 \cong 0$$

$$C_{mi} = \frac{4.6}{1080 \text{ kip in.}} = 0.004 \cong 0$$

F. S. = 2.7

(c) $Q_{allowable}$

$$Q_{allowable} = \frac{Quc}{F.S.} = \frac{6110}{2.7} = 2260 \text{ lb}$$

Specimen Design

1. Computation of M_p.—The proportions of the composite section (Fig. 8) are such that the neutral axis is located in the slab at ultimate. The steel section is completely yielded in tension and the concrete is assumed to have no tensile resistance. The internal couple method is used in computing the plastic moment.

The total tensile force T developed by the steel section is

$$T = f_y \ A_s = 37.0 \times 5.00 = 185 \text{ kips}$$

For longitudinal equilibrium, a compressive force equal in magnitude to this tensile force in the steel is required. It is assumed that this compressive force is provided by an area of concrete fully stressed to the cylinder strength f_c'. The depth of penetration of this compressive area into the slab is

$$d_p = \frac{T}{f_c' \ b_c} = \frac{185}{24.5500} = 1.40 \text{ in.}$$

The moment arm between the tensile and compressive forces is

$$e = 4.0 + 3.0 - \frac{1.40}{2} = 6.30 \text{ in.}$$

The plastic moment of the composite section is the moment produced by this couple of tensile and compressive forces

$$M_p = T \ e = 185 \times 6.30 = 1165 \text{ kip - in.}$$

2. Computation of shear flow.—The shear flow is computed by taking a free body of the slab between the section of full plastic moment and zero moment (Fig. 9). The length is denoted by L_s.

Spacing 1 (Test 1) 2 b = 24 in.

$$P_p = \frac{M_p}{24} = \frac{1165}{24} = 48.5 \text{ kips}$$

$$S_p = \frac{C}{\frac{L}{2} - 12} = \frac{185}{60 - 12} = 3.85 \text{ kips per in.}$$

TABLE 6.—VALUES OF 2 b, P_p AND S_p.

Spacing (1)	2 b, in in. (2)	P_p, in kips (3)	S_p, in kips per in. (4)
1	24	48.5	3.85
2	36	55.5	4.40
3	46	63.0	5.00

TABLE 7.—TEST RESULTS

Beam (1)	Test 1		Test 2		Test 3	
	Force per stud, in kips (2)	τ, in kips per sq in. (3)	Force per stud, in kips (4)	τ, in kips per sq in. (5)	Force per stud, in kips (6)	τ, in kips per sq in. (7)
B-1	7.05	35.9	...	...	...	...
B-2	10.6	54.0	12.1	61.7	...	...
B-3	13.4	68.4	15.4	78.5	17.5	89.1

3. Computation of connector forces.—By assuming that the connector forces are equal over the length L_s, the connector forces are computed by multiplying the shear flow by the connector spacing.

$$Q = \frac{s\ S_p}{c} \text{ (force per stud)}$$

B - 1 (3 studs per row at 5.5 in.)

$$Q = \frac{5.5 \cdot 3.85}{3} = 7.05 \text{ kips}$$

τ = 35.9 kips per sq in.
(average shearing stress in stud)

4. Fatigue specimen.—The fatigue specimen was designed so that the shear stress on the studs would approach the fatigue strength based on a fatigue life of 2×10^6 cycles, obtained in previous pushout tests. This was achieved by setting the maximum fiber stress in the stud section at 30 kips per sq in.

Maximum fiber stress in WF section = 30 kips per sq in.

$$f_s = \frac{M a_{st}}{I} = M = \frac{(30)\ 151.3}{7.25} = 625 \text{ kip - in.}$$

$$P = \frac{M}{21} = \frac{625}{21} = 29.8 \text{ kips}$$

$$V = 15.0 \text{ kips}$$

$$S = \frac{V_m}{I} = \frac{(15.0)\ 16.2}{151.3} = 1.60 \text{ kips per in.}$$

$$Q = \frac{(1.60)\ 5.5}{3} = 2.94 \text{ kips}$$

$$\tau = \frac{2.94}{0.196} = 15 \text{ kips per sq in.}$$

Deflection Computations.—The theoretical deflections of the static specimen in the elastic range consists of deflection due to bending and shearing deflection. A sample of the computations involved follows:

1. Static deflections
   (a) Due to bending

$$\delta_B = \frac{P a}{24 E I} \left(3 L^2 - 4 a^2\right)$$

in which

$$L = 10 \text{ ft}$$
$$E = 30 \times 10^3 \text{ kips per sq in.}$$
$$I = 151.3 \text{ in.}^4$$
$$a = \begin{cases} \text{T1} - 48 \text{ in.} \\ \text{T2} - 42 \text{ in.} \\ \text{T3} - 37 \text{ in.} \end{cases}$$

   (b) Due to shear

$$\delta_s = \frac{\tau a}{G} = \frac{P a}{2 A_w G}$$

in which

$$A_w = 1.84 \text{ sq in. (web area of steel beam)}$$
$$G = 11.5 \times 10^3 \text{ kips per sq in.}$$

   (c) Total static deflection

$$\delta = \delta_B + \delta_s$$

TABLE 8.—DEFLECTIONS

Deflection	T1	T2	T3
	Load P, in kips		
	30	30	40
Deflection due to Bending δ_B in in.	0.224	0.208	0.256
Deflection due to Shear δ_s, in in.	0.034	0.030	0.035
Total Deflection $\delta_B + \delta_s$, in in.	0.258	0.238	0.291

APPENDIX II.—NOTATION

A_s = steel area;

a_{st} = distance from neutral axis of composition section to extreme fiber of of steel in tension;

b = distance from center line of beam to point of load;

b_c = effective width of concrete slab;

C = total compressive force = $f'_c\, b_c\, d_p$;

c = number of connectors per transverse row;

d_c = depth of concrete slab;

d_p = depth of compressive stress block at M_p;

d_s = depth of steel section;

e = distance between resultant compression and tension forces at M_p;

f_c = concrete stress;

f'_c = cylinder strength of concrete at 28 days;

f_s = steel stress;

f_y = yield stress of steel beam;

I = moment of inertia of composite section, concrete transformed to equivalent steel area;

I_s = moment of inertia of steel section;

L_s = shear span = distance between sections at which plastic moment and zero moment occur;

m = statical moment of transformed compressive concrete area about the neutral axis of the composite section;

M_p = theoretical plastic moment of composite section;

M_u = experimentally observed ultimate moment;

M_y = theoretical yield moment;

$n = \frac{E_{steel}}{E_{concrete}}$;

P = externally applied load;

P_p = externally applied load at M_p;

P_u = externally applied load at M_u;

P_y = externally applied load at M_y;

Q = connector force;

s = connector spacing along longitudinal axis of beam;

S = shear flow per unit length at interface of slab and steel beam;

S_p = shear flow at M_p;

T = total tensile force = $f_y \ A_s$;

V = shear force;

δ = deflection of beam, in inches; and

δ_r = residual deflection of beam, in inches.

Journal of the
STRUCTURAL DIVISION
Proceedings of the American Society of Civil Engineers

DISCUSSION

Note.—This paper is a part of the copyrighted Journal of the Structural Division, Proceedings of the American Society of Civil Engineers, Vol. 87, No. ST 2, February, 1961.

BAR-CHAIN METHOD FOR ANALYZING TRUSS DEFORMATION[a]

Discussion by Chun-Yeh Liu

CHUN-YEH LIU.[15]—The authors are to be commended for applying the bar-chain method to the analysis of statically determinate and indeterminate trusses. Because this method, according to the authors, is "analogous to the conjugate frame method for analyzing the deformation of continuous frames; the conjugate frame method is an extension of the conjugate beam method," it appears that the analysis for computing truss deformation is based on the application of the conjugate-beam procedure. However, their sign convention of bar chains for the vertical and horizontal deflection components does not seem to follow the usual sign convention given for the conjugate beam.

Because the relationship between the conjugate beam and the actual beam is similar to that which exists between the conjugate bar chain and the actual bar chain, the writer, therefore, is rather inclined to follow the same sign convention and principles as those used in the conjugate beam, because they are convenient, automatic, and easy to remember. Adopting the usual sign convention for the conjugate beam, the sign convention for bar chains can be stated as follows:

In the actual bar chain, the vertical component of joint deflection is positive if the joint moves downward, and the rotation is positive if it lends to rotate the joint clockwise. For the horizontal component of joint deflection, the same convention can be used if the actual bar chain is to be viewed from the right-hand side of the computation sheet. For example, in Fig. 2(a), the end a of the actual bar chain abc is then the right end.

In the conjugate bar chain for the vertical deflection component, following the usual beam convention for shear and moment, positive elastic weights act downward. Positive bending moment and positive shear on the conjugate bar chain correspond to the downward deflection and clockwise equivalent rotation of the actual bar chain, respectively. It is interesting to note that actually one has one's correspondence in the conjugate and actual bar chain. For the horizontal deflection component, the same convention can be used, if the conjugate bar chain is to be viewed from the right-hand side of the computation sheet. For example, in Fig. 2(d), the end a of the conjugate bar chain abc is then the right end.

Thus, the conjugate bar chain abc for the horizontal deflection components as originally shown in Fig. 2(d) that correspond to the displacement of the actual bar chain abc as shown in Fig. 2(a) is represented by a figure in which

---

[a] May 1960, by S. L. Lee and P. C. Patel (Proc. paper 2477).

[15] Prof., Dept. of Agric. Engrg., Natl. Taiwan Univ., Taipei, Taiwan, China.

the arrows for δ_{ax} and δ_{cx} in Fig. 2(d) are reversed. Eq. 16 thus would be changed to

$$W_{bx} = \delta\beta - \delta\beta' + e\cot\beta - e'\cot\beta' \ldots\ldots\ldots (28)$$

As the right-hand side of the conjugate bar chain as shown in the revised Fig. 2(d) is considered as the 'lower side' in applying the beam convention and the same conjugate bar chain is subjected to the horizontal elastic weight, W_{bx}, to the right and supported at the ends by positive 'bending moments' δ_{ax} and δ_{cx} and 'shearing forces' θ_{ax} and θ_{cx}, it is obvious that $\delta\beta - \delta\beta'$ in Eq. 16 is the angle measured below the bar chain of the revised Fig. 2(d), as viewed from the right-hand side of the computation sheet.

It is to be noted that in so doing, the determination of the vertical and horizontal components of joint deflection and equivalent rotation of the actual bar chain can be simplified to the mere computation of the corresponding bending moment and shear of the conjugate bar chain, respectively, that is so familiar to the structural engineer and, through the use of the usual beam convention, errors in application are almost impossible.

JAMES CHINN,[16] M. ASCE.—Messrs. Lee and Patel have extended an elastic-weights method used by some engineers for computing frame deflections so that it can be used for trusses.

The method consists of assuming rotations to be loads on a conjugate structure, acting horizontally for horizontal deflections and vertically for vertical deflections. For the truss, some artifice must be used to account for length changes of members.

A. C. Scordelis, M. ASCE and C. M. Smith presented a conjugate-structure method[17] for solving truss deflections that the writer used for several years. This method is similar to the column analogy in that angle changes are considered as loads acting perpendicular to the plane of a conjugate structure. Shears in the conjugate structure then represent rotations, moment about a vertical axis represents vertical deflection, and moment about a horizontal axis represents horizontal deflection.

The method for frames, considering bending deflections only is illustrated in Fig. 7. The sign conventions used by the writer are:

1. Moment convention is the bending sign convention, that is, tension on the bottom fibers of a beam or on the inside fibers of a frame is positive.
2. Positive moment is a downward load on the conjugate structure.
3. Shear on the conjugate structure is viewed from the bottom in beams and from the inside of frames. Shear acting clockwise on the free body represents clockwise rotation.
4. The vector representing moment in the conjugate structure points in the direction of deflection as it acts on the left-hand free body.

---

16 Prof. of Civ. Engrg., Univ. of Colorado, Boulder, Colo.

17 "An Anlytical Procedure for Calculating Truss Displacements," by A. C. Scordelis and C. M. Smith, Vol. 81, Proceedings, ASCE, July, 1955.

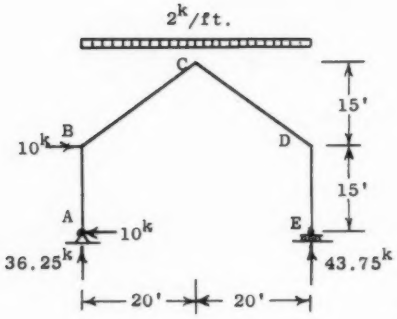

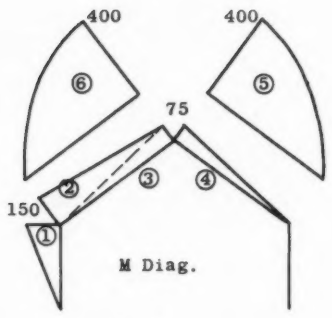

Areas

①	(1/2)(150)(15) = 1125
②	(1/2)(150)(25) = 1875
③ - ④	(1/2)(75)(25) = 937.5
⑤ - ⑥	(2/3)(400)(25) = 6666.7

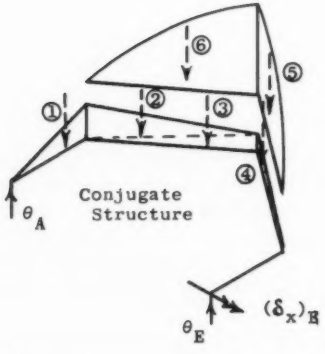

Denotes moment vector

Taking moments about DE:

$$40\theta_A = 40(1125) + 1875(20 + \tfrac{2}{3}\,20) + 937.5(20 + \tfrac{1}{3}\,20) + 6666.7(20 + \tfrac{3}{8}\,20) + 6666.7(\tfrac{5}{8}\,20) + 937.5(\tfrac{2}{3}\,20)$$

$$\theta_A = 10{,}291.7/EI \quad \text{clockwise}$$

FIG. 7.—EXAMPLE A

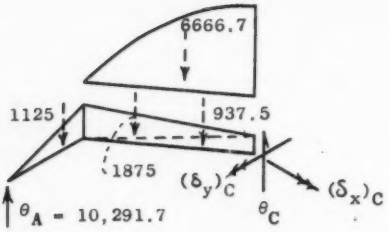

Summing forces:

$$\theta_C = 1125 + 1875 + 937.5 + 6666.7 - 10,291.7$$
$$= 312.5/EI \text{ c-clockwise}$$

Taking moments about a y-axis through C:

$$(\delta_y)_C = 10,291.7(20) - 1125(20) - 1875(\tfrac{2}{3}\ 20) - 937.5(\tfrac{1}{3}\ 20) - 6666.7(\tfrac{3}{8}\ 20)$$
$$= 102,084/EI \text{ downward}$$

Taking moments about an x-axis through C:

$$(\delta_x)_C = 10,291.7(30) - 1125(15 + \tfrac{15}{3}) - 1875(\tfrac{2}{3}\ 15) - 937.5(\tfrac{1}{3}\ 15) - 6666.7(\tfrac{3}{8}\ 15)$$
$$= 225,313/EI \text{ to the right}$$

FIG. 7.—*CONTINUED*

Axial deformations can be taken into account as moment loadings represented by vectors along the members. The writer always works left to right, so the vector load on a member must act in a direction opposite to the relative motion of the "right" end of the member with respect to the "left." Concentrated angle changes at hinges are positive or negative concentrated loads on the conjugate structure according to whether they would be caused by positive or negative bending.

The authors' example 1 is solved by the conjugate-structure method in Fig. 8. A comparison of the two methods can be made from the two examples. In the Scordelis-Smith method, the axial deformation is represented by a moment vector along the member. In computing vertical deflections, only the vertical component of this vector is involved, and in computing horizontal deflections, only the horizontal component.

The vertical component can also be represented by a couple with a horizontal arm. For example, for member $L_0\ U_1$, the vertical component of the 79.8

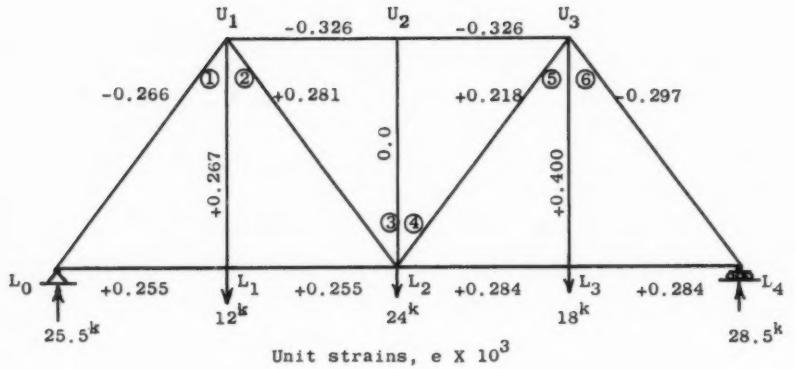

Unit strains, e X 10^3

Calculation of angle changes

$\Delta\chi = (e_{opposite} - e_{right})\cot\chi_{right} + (e_{opposite} - e_{left})\cot\chi_{left}$

① (0.255 + 0.266)(0.75) + (0.255 - 0.267)(0) = 0.39075
② (0.255 - 0.267)(0) + (0.255 - 0.281)(0.75) = -0.01950 } 0.37125

③ (-0.326 - 0)(0) + (-0.326 - 0.281)(0.75) = -0.45525
④ (-0.326 - 0.218)(0.75) + (-0.326 - 0)(0) = -0.40800 } -0.86325

⑤ (0.284 - 0.218)(0.75) + (0.284 - 0.400)(0) = 0.04950
⑥ (0.284 - 0.400)(0) + (0.284 + 0.297)(0.75) = 0.43575 } 0.48525

Calculation of length changes

ΔL = e X length of member

ΔU_1L_0 = -0.266(25)(12) = -79.8

ΔU_1L_2 = 0.281(25)(12) = 84.3

ΔU_3L_2 = 0.218(25)(12) = 65.4

ΔU_3L_4 = -0.297(25)(12) = -89.1

FIG. 8.—EXAMPLE B

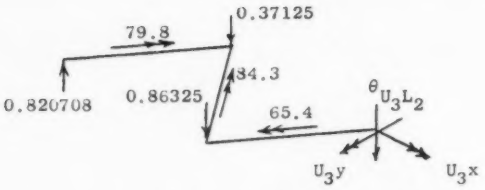

Taking moments about an x-axis through U_3:

$$\delta_{U_3x} - (0.820708 - 0.86325)(240) - \frac{3}{5}(65.4 + 84.3 - 79.8) = 0$$

$$\delta_{U_3x} = 31.73 \times 10^{-3} \text{ ins. to the right}$$

Taking moments about a y-axis through U_3:

$$\delta_{U_3y} - 0.820708(540) + 0.37125(360) + 0.86325(180) + \frac{4}{5}(65.4 - 84.3 - 79.8) = 0$$

$$\delta_{U_3y} = 233.1 \times 10^{-3} \text{ ins. downward}$$

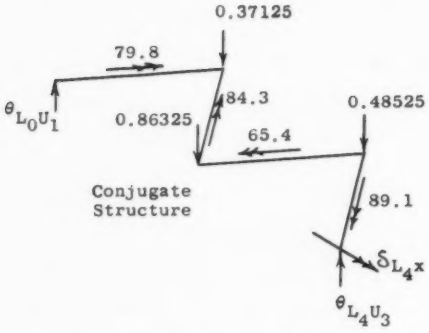

Taking moments about a y-axis through L_4:

$$720\ \theta_{L_0U_1} - 540(0.37125) - 360(0.86325) - 180(0.48525) + \frac{4}{5}(79.8 + 84.3 - 65.4 - 89.1) = 0$$

$$\theta_{L_0U_1} = 0.820708$$

Taking moments about an x-axis through L_4:

$$\delta_{L_4x} - (0.37125 + 0.48525)(240) + \frac{3}{5}(79.8 + 89.1 - 84.3 - 65.4) = 0$$

$$\delta_{L_4x} = 194.2 \times 10^{-3} \text{ ins. to the right}$$

FIG. 8. —*CONTINUED*

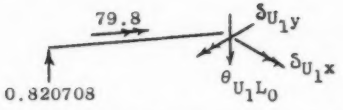

Taking moments about an x-axis through U_1:

$$\delta_{U_1x} - 0.820708(240) + \frac{3}{5}(79.8) = 0$$

$$\delta_{U_1x} = 149.1 \times 10^{-3} \text{ ins. to the right}$$

Taking moments about a y-axis through U_1:

$$\delta_{U_1y} - 0.820708(180) - \frac{4}{5}(79.8) = 0$$

$$\delta_{U_1y} = 211.6 \times 10^{-3} \text{ ins. downward}$$

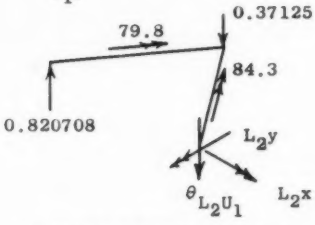

Taking moments about an x-axis through L_2:

$$\delta_{L_2x} - 0.37125(240) + \frac{3}{5}(79.8 - 84.3) = 0$$

$$\delta_{L_2x} = 91.8 \times 10^{-3} \text{ ins. to the right}$$

Taking moments about a y-axis through L_2:

$$\delta_{L_2y} - 0.820708(360) + 0.37125(180) - \frac{4}{5}(79.8 + 84.3) = 0$$

$$\delta_{L_2y} = 359.9 \times 10^{-3} \text{ ins. downward}$$

FIG. 8.—*CONTINUED*

vector is 0.8(79.8) = 63.84. This can be represented by equal and opposite forces of 63.84/180 = 0.35467 with a horizontal distance of 180 in. (15 ft) between them. Similarly, the vertical component of the 84.3 vector can be represented by forces of (0.8) 84.3/180 = 0.37467, etc. For computing vertical deflections, the loads of Fig. 9(b) are equivalent to those of Fig. 8, the true conjugate structure. In a similar way, splitting the horizontal components of moment vectors into couples with vertical moment arms, the loads of Fig. 9(d) are equivalent to those of Fig. 8 for computing horizontal deflections.

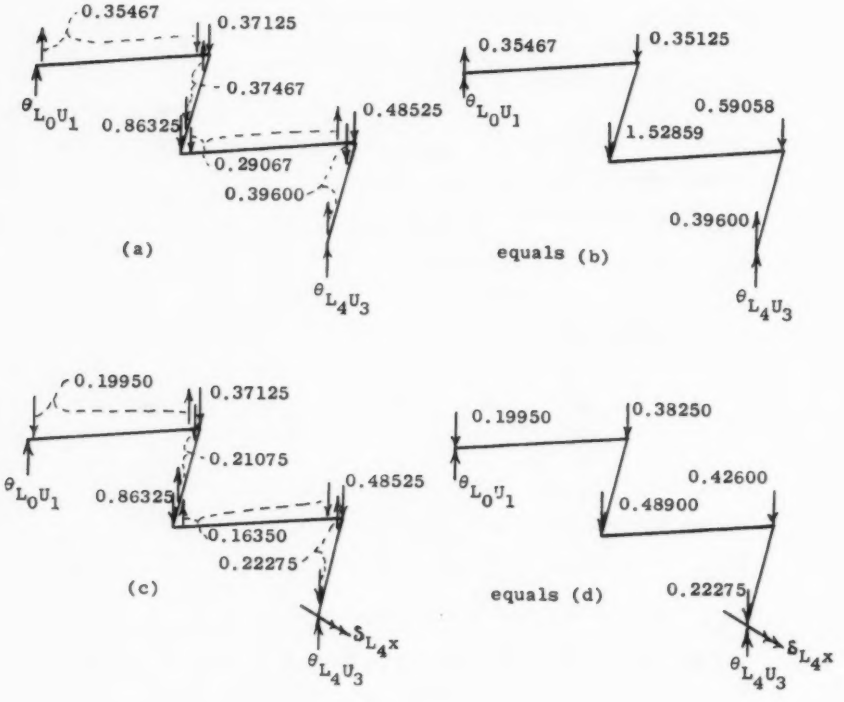

FIG. 9

If the loads of Fig. 9(b) are "flopped" over to act vertically in the plane of the structure, the Fig. 3(b) is obtained, and if the loads of Fig. 9(d) are "flopped" over to act horizontally in the plane of the structure, Fig. 3(c) is obtained.

INFLUENCE OF PARTIAL BASE FIXITY ON FRAME STABILITY[a]

Discussion by Joseph W. Appeltauer and Thomas A. Barta

J. W. APPELTAUER,[17] and TH. A. BARTA.[18]—As Galambos points out in his paper, partial base fixity may be studied either by inserting a restraining beam between the column bases, a method used also by other authors (for example, Kornouhov,[19] Goder[20]), or by considering directly the end rotations.

In their research on framework stability, the results of which are due to be published in the Bulletin of the Building Research Institute (Bucharest), the authors resolved, among others, the problem of partial base fixity for different current frameworks by using the "degree of restraint (degree of fixity) ϵ." The degree of restraint is the ratio of the partial-base-restraint moment versus the corresponding fixed-base moment, under the action of a unit moment, acting on the opposite end of the columns. The extreme values of the degree of restraint are $\epsilon = 0$, for a pinned base, and $\epsilon = 1$, for a fixed base. With

$$\delta = \frac{E_t I_c}{L_c} \phi \quad \ldots\ldots\ldots\ldots\ldots\ldots \quad (53)$$

in which ϕ is the rotation of the foundation under the action of a unit moment there results

$$\epsilon = \frac{1}{1 + 3\delta} \quad \ldots\ldots\ldots\ldots\ldots\ldots \quad (54)$$

The rotation ϕ may be determined by

$$\phi = \frac{12}{g\, q\, f^3} \quad \ldots\ldots\ldots\ldots\ldots\ldots \quad (55)$$

that represents the reciprocal of Mr. Galambos' Eq. 37.

Further data on the degree of restraint ϵ, respectively the coefficient q, is available.[21,22,23] The rotation of the base due to the deformation of the anchor-

---

[a] May 1960, by T. V. Galambos (Proc. paper 2480).

[17] Civ. Engr., Timisoara, Rumania.

[18] Civ. Engr., Timisoara, Rumania.

[19] "Protchnost i ustoichivost starshnavyi system," by N. V. Kornouhov, Stroyisdat, Moscow, 1948.

[20] "Beitrag zur praktischen Berechnung von Rahmentragwerken nach der Stabilitätsvorschrift DIN 4114," by W. Goder, Stahlbau, Vol. 28, No. 10, October, 1959, p. 265.

[21] "The Problem of Partial Restraint in Elastic Soil," (in Rumanian) by C. N. Avram, Institutul Politehnic Timisoara, Buletinul Comunicarilor Stiintifice si Tehnice Vol. 1, 1956.

[22] "Mehanika gruntov," by N. A. Tsytovitch, Stroyisdat, Moscow, 1951. (Rumanian translation -ESAC, Bucharest, 1955).

[23] "Über den Einepanngrad einer Stütze im Fundament," by K. Opladen, Beton- u. Stahlbetonbau, Vol. 55, No. 2, February, 1960, p. 35.

bolts and the concrete, has been treated also by P. Sahmel,[24] and contrary to Mr. Galambos' statement should be added to the rotation of the foundation.

It is interesting to mention that in European practice, columns like these described by Mr. Galambos are considered, for simplicity, as having fixed ends, so that partial base fixity reduces the rigidity of the base. Moreover, this hypothesis is confirmed by Mr. Galambos' numerical example.

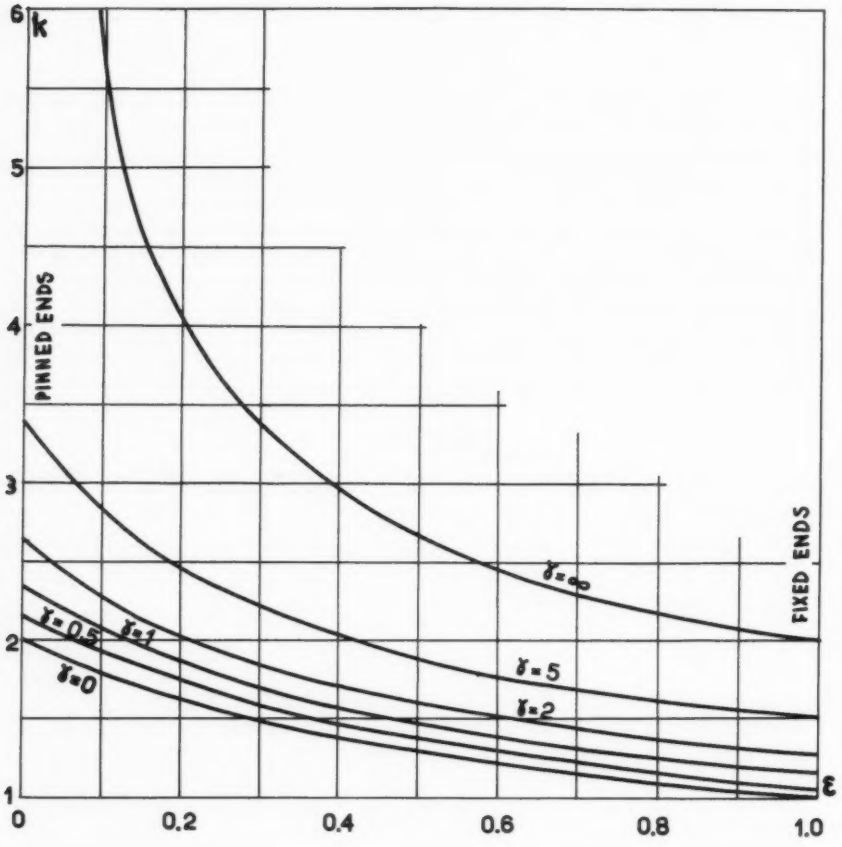

FIG. 12.—EFFECTIVE LENGTH OF COLUMNS IN A SINGLE-STORY SINGLE-BAY FRAME

The Single-Story, Single-Bay Frame.—It is interesting and useful to write the stability equation and to represent its results using the degree of restraint

24 "Näherungsweise Berechnung der Knicklängen von Stockwerkrahmen," by P. Sahmel, Stahlbau, Vol. 24, No. 4, April, 1955, p. 89.

as a parameter. The stability equation for the geometrically and mechanically symmetric frame is:

$$(1-\epsilon)\left(1-\frac{\gamma}{6}\,\phi\tan\phi\right)+3\,\epsilon\left(\frac{\tan\phi}{\phi}+\frac{\gamma}{6}\right)=0 \quad \ldots\ldots\ldots\ldots (56)$$

Figs. 12 and 13 correspond with Figs. 5 and 6. In comparing these figures, the

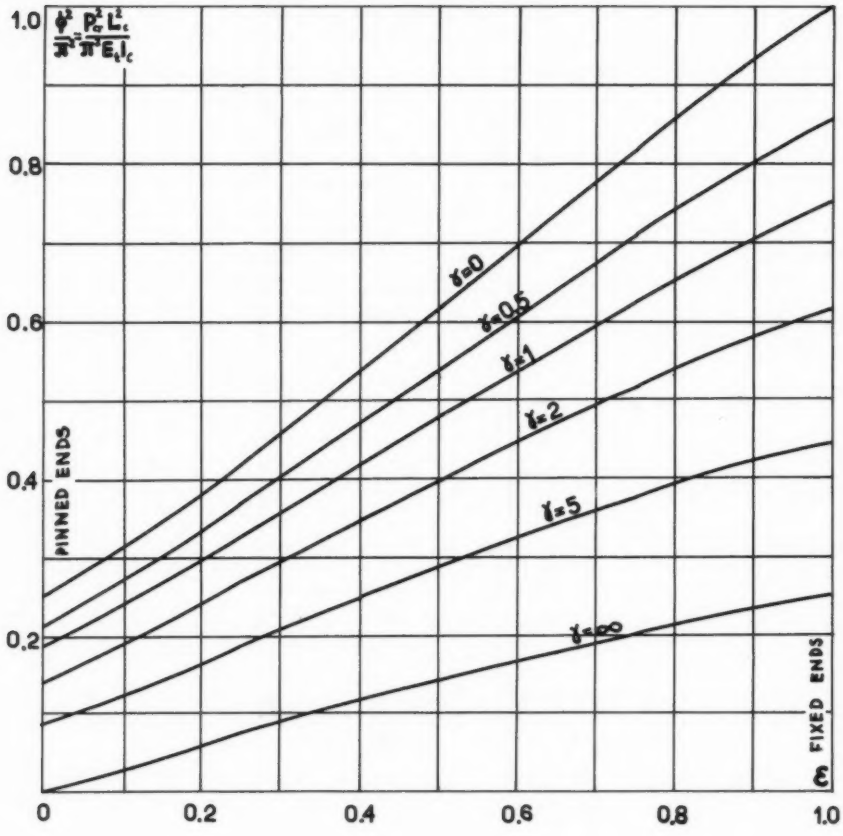

FIG. 13.—VARIATION OF CRITICAL LOAD WITH BASE RESTRAINT FOR A SINGLE-STORY SINGLE-BAY FRAME

advantage of the degree of restraint ϵ versus the coefficient of restraint λ can be seen, as the latter very much shortens the first half ($0\leq\epsilon\leq 0.5$ respectively, $0\leq\lambda\leq 0.5$) of the interval, and lengthens unnecessarily the second ($0.5\leq\epsilon\leq 1$ respectively $0.5\leq\lambda\leq\infty$). This distortion of the scale explains also the pronounced slope of the curves in the interval $0\leq\lambda\leq 0.5$.

For $0 \leq \gamma \leq 2.5$ may be used the approximate formula

$$k = \sqrt{\frac{1+m}{2}} \sqrt{\frac{4(2+\gamma')-2\epsilon}{2+\epsilon(4+\gamma')}} \quad \ldots\ldots\ldots\ldots\ldots\ldots \quad (57)$$

in which $\gamma' = \frac{\pi^2}{12}\gamma \sim 0.822\,\gamma$ and $m \leq 1$ is the ratio of the two forces acting in the

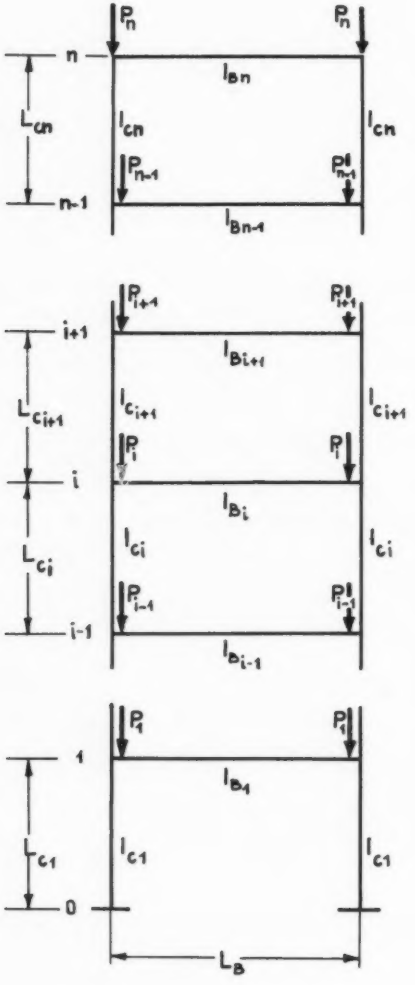

FIG. 14.—MULTI-STORY FRAME

columns. In the particular case of a frame with a beam connected by pins to the columns ($\gamma = \infty$) the approximate formula

$$k = \frac{2}{3}\,\frac{1+2\epsilon}{\epsilon}\left[1-\frac{2}{3}\left(\frac{1-\epsilon}{1+2\epsilon}\right)^3\right] \quad \ldots\ldots\ldots\ldots\ldots\ldots \quad (58)$$

may be used. Eq. 57 has been derived using the "equilibrium-method" and Eq. 58 by the approximate solution of the stability equation

$$\phi \tan \phi - \frac{3\,\epsilon}{1-\epsilon} = 0 \quad \ldots\ldots\ldots\ldots\ldots\ldots \quad (59)$$

Multi-Story and Multi-Bay Frames.—For a symmetrical single-bay, multi-story frame, with n stories (Fig. 14) the following approximative formula may be used

$$k_n^2 = \frac{\bar{f}_1\left[2^{n-1}\,\xi'^2\,\frac{L'_{c_s}}{L_{c_n}}\sum_{1}^{n} p\text{-}2^{n-2}\,\frac{L'_{c_s}}{L_{c_n}}\sum_{2}^{n} p\right] + \sum_{2}^{n}\bar{f}_i\left[2^{n-i}\,\frac{L'_{c_i}}{L_{c_n}}\sum_{i}^{n} p\text{-}2^{n-(i+1)}\,\frac{L'_{c_{i+1}}}{L_{c_n}}\sum_{i+1}^{n} p\right]}{2^{n-1}\,n\,\xi'^2\,\frac{L_{c_s}}{L_{c_n}}\,\frac{L'_{c_s}}{L_{c_n}} + \sum_{2}^{n} 2^{n-i}(n-i+1)\,\frac{L_{c_i}}{L_{c_n}}\,\frac{L'_{c_i}}{L_{c_n}}} \quad \ldots \quad (60)$$

with the notations

$$L'_{c_i} = L_{c_i}\,\frac{E_{t_n}\,I_{c_n}}{E_{t_i}\,I_{c_i}}\,;\quad \xi' = \frac{2+\epsilon}{2(1+2\epsilon)}\,;\quad p_i = \frac{P_i}{P_n}$$

The reduced deflections $\bar{f}_i$ of Eq. 60 result from the recurrence formulas:

$$\bar{f}_1 = 4n\left(3\xi^2-3\xi+1\right)\left(\frac{L_{c_s}}{L_{c_n}}\right)^2\frac{L'_{c_s}}{L_{c_n}} + 1{,}644\,\xi'\,\frac{L\,B_s}{L_{c_n}}\,\frac{L_{c_s}}{L_{c_n}}\,\frac{n\xi'\,L_{c_s}+\frac{n-1}{2}\,L_{c_2}}{L_{c_n}} + 4n\,\frac{1-\epsilon}{\epsilon}\,\xi^2\left(\frac{L_{c_s}}{L_{c_n}}\right)^2\frac{L'_{c_s}}{L_{c_n}} \quad \ldots \quad (61)$$

$$\bar{f}_2 = \bar{f}_s + (n-1)\left(\frac{L_{c_2}}{L_{c_n}}\right)^2\frac{L'_{c_2}}{L_{c_n}} + 0.822\,\frac{L'_{B_s}}{L_{c_n}}\,\frac{L_{c_2}}{L_{c_n}}\,\frac{n\xi'\,L_{c_s}+\frac{n-1}{2}\,L_{c_2}}{L_{c_n}} + 0.822\,\frac{L'_{B_2}}{L_{c_n}}\,\frac{L_{c_2}}{L_{c_n}}\,\frac{\frac{n-s}{2}\,L_{c_2}+\frac{n-2}{2}\,L_{c_3}}{L_{c_n}} \quad \ldots \quad (62)$$

$$\begin{aligned}\bar{f}_i = \bar{f}_{i-1} &+ (n-i+1)\left(\frac{L_{c_i}}{L_{c_n}}\right)^2\frac{L'_{c_i}}{L_{c_n}} \\ &+ 0.822\,\frac{L'_{B_{i-s}}}{L_{c_n}}\,\frac{L_{c_i}}{L_{c_n}}\,\frac{\frac{n-i+2}{2}\,L_{c_{i-s}}+\frac{n-i+1}{2}\,L_{c_i}}{L_{c_n}} \\ &+ 0.822\,\frac{L'_{B_i}}{L_{c_n}}\,\frac{L_{c_i}}{L_{c_n}}\,\frac{\frac{n-i+1}{2}\,L_{c_i}+\frac{n-i}{2}\,L_{c_{i+1}}}{L_{c_n}} \quad \ldots\ldots\ldots \quad (63)\end{aligned}$$

$$\bar{f}_n = \bar{f}_{n-1} + 1 + 0.411\,\frac{L'_{B_{n-s}}}{L_{c_n}}\left(2\,\frac{L_{c_{n-1}}}{L_{c_n}}+1\right) + 0.411\,\frac{L'_{B_n}}{L_{c_n}} \quad \ldots\ldots\ldots \quad (64)$$

with the supplementary notations

$$L'_{B_i} = L_{B_i}\,\frac{E_{t_n}\,I_{c_n}}{E_{B_i}\,I_{B_i}}\,;\quad \xi = 1{,}5\,\frac{\epsilon}{1+2\,\epsilon} = 1-\xi'$$

The effective-length coefficients for the other columns may be computed from

$$k_i^2 = \frac{k_n^2}{\frac{L_{c_i}}{L_{c_n}} \frac{L'_{c_i}}{L_{c_n}} \sum_i^n p} \quad \ldots\ldots\ldots\ldots\ldots\ldots (65)$$

For the particular case of a three-story frame, Eqs. 60 through 65 yield

$$k_3^2 = \frac{\bar{f}_1\left[4\xi'^2 \frac{L'_{c_s}}{L_{c_3}}(p_s+p_2+1) - 2\frac{L'_{c_2}}{L_{c_3}}(p_2+1)\right] + \bar{f}_2\left[2\frac{L'_{c_2}}{L_{c_3}}(p_2+1) - 1\right] + \bar{f}_3}{12\,\xi'^2 \frac{L_{c_s}}{L_{c_3}} \frac{L'_{c_s}}{L_{c_3}} + 4\frac{L_{c_2}}{L_{c_3}} \frac{L'_{c_2}}{L_{c_3}} + 1} \quad \ldots\ldots (66)$$

$$k_2^2 = \frac{k_3^2}{\frac{L_{c_2}}{L_{c_3}} \frac{L'_{c_2}}{L_{c_3}}(p_2+1)} \quad \ldots\ldots\ldots\ldots\ldots\ldots (67)$$

$$k_s^2 = \frac{k_3^2}{\frac{L_{c_s}}{L_{c_3}} \frac{L'_{c_s}}{L_{c_3}}(p_s+p_2+1)} \quad \ldots\ldots\ldots\ldots\ldots\ldots (68)$$

$$\bar{f}_1 = 12(3\xi^2-3\xi+1)\left(\frac{L_{c_s}}{L_{c_3}}\right)^2 \frac{L'_{c_s}}{L_{c_3}} + 1.644\xi' \frac{L'_{B_s}}{L_{c_3}} \frac{L_{c_s}}{L_{c_3}} \frac{3\xi' L_{c_s}+L_{c_2}}{L_{c_3}}$$

$$+12\frac{1-\epsilon}{\epsilon}\xi^2\left(\frac{L_{c_s}}{L_{c_3}}\right)^2 \frac{L'_{c_s}}{L_{c_3}} \quad \ldots\ldots\ldots\ldots (69)$$

$$\bar{f}_2 = \bar{f}_1 + 2\left(\frac{L_{c_2}}{L_{c_3}}\right)^2 \frac{L'_{c_2}}{L_{c_3}} + 0.822 \frac{L'_{B_s}}{L_{c_3}} \frac{L_{c_2}}{L_{c_3}} \frac{3\xi' L_{c_s}+L_{c_2}}{L_{c_3}}$$

$$+0.411 \frac{L'_{B_2}}{L_{c_3}} \frac{L_{c_2}}{L_{c_3}} \left(2\frac{L_{c_2}}{L_{c_3}}+1\right) \quad \ldots\ldots\ldots\ldots (70)$$

$$\bar{f}_3 = \bar{f}_2 + 1 + 0.411 \frac{L'_{B_2}}{L_{c_3}} \left(2\frac{L_{c_2}}{L_{c_3}}+1\right) + 0.411 \frac{L'_{B_3}}{L_{c_3}} \quad \ldots\ldots\ldots\ldots (71)$$

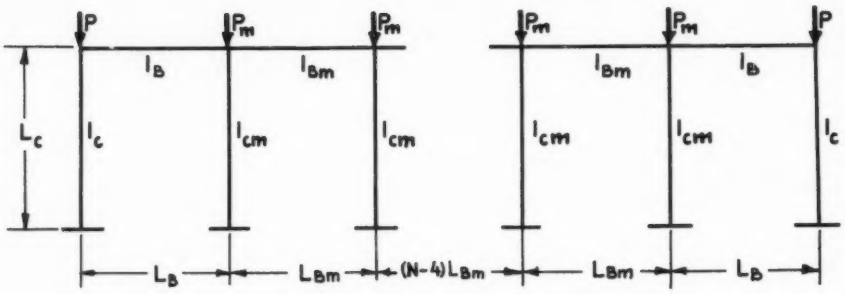

FIG. 15.—MULTI-BAY FRAME

For a symmetrical single-story, multi-bay frame, with N bays (Fig. 15) the approximate formula for the effective length of the marginal column, may be used:

$$k^2 = \bar{f}\,\frac{m\xi'^2 + (N-1)p_m\xi'^2_m}{m\xi'^2 + 2(N-1)\,\xi'^2_m} \qquad (72)$$

The reduced deflection is

$$\bar{f} = \frac{4}{N}\left[\left(3\xi^2 - 3\xi + 1\right) + \frac{2(N-1)}{m}\left(3\xi_m^2 - 3\xi_m + 1\right) + 0.822\,\frac{L'_B}{L_c}\left(\xi'^2 - \xi'\,\xi'_m + \xi'^2_m\right)\right.$$

$$\left. + 0.411(N-2)\,\frac{L'_{B_m}}{L_c}\,\xi'^2_m + \frac{1-\epsilon}{\epsilon}\,\xi^2 + \frac{2(N-1)}{m}\,\frac{1-\epsilon_m}{\epsilon_m}\,\xi^2_m\right] \qquad (73)$$

with the new notations

$$m = \frac{E_{t_m}\,I_{c_m}}{E_t\,I_c}\;;\quad \xi_m = 1.5\,\frac{\epsilon_m}{1+2\,\epsilon_m}\;;\quad \xi'_m = 1-\xi_m\;;\quad p_m = \frac{P_m}{P}$$

The effective-length coefficient for an intermediate column is

$$k_m^2 = k^2\,\frac{m}{p_m} \qquad (74)$$

For a symmetrical multi-story, multi-bay frame, with N bays and n stories may be used the approximate formula

$$k_n^2 = \left(\bar{f}_1 \left/ \right. 2^{n-1}\xi'^2\,\frac{L'_{c_s}}{L_{c_n}}\sum_{\bar{1}}^{n} p + 2^{n-2}\,\frac{L'_{c_2}}{L_{c_n}}\sum_{\bar{2}}^{n} p + (N-1)\left[2^{n-1}\xi'^2_m\,\frac{L'_{c_{m_s}}}{L_{c_n}}\sum_{\bar{1}}^{n} p_m + 2^{n-2}\,\frac{L'_{c_{m_2}}}{L_{c_n}}\sum_{\bar{2}}^{n} p_m\right] \Big/ \right.$$

$$\left. + \sum_{\bar{2}}^{n}\bar{f}_i \left/ \right. 2^{n-i}\,\frac{L'_{c_i}}{L_{c_n}}\sum_{\bar{1}}^{n} p + 2^{n(i+s)}\,\frac{L'_{c_{i+1}}}{L_{c_n}}\sum_{\bar{i+s}}^{n} p + (N-1)\left[2^{n-i}\,\frac{L'_{c_{m_i}}}{L_{c_n}}\sum_{\bar{1}}^{n} p_m + 2^{n-(i+1)}\,\frac{L'_{c_{m_{i+1}}}}{L_{c_n}}\sum_{\bar{i+1}}^{n} p_m\right] \Big/ \right) \qquad (75)$$

$$\div \left(2^{n-1}\xi'^2\,\frac{L_{c_1}}{L_{c_n}}\,\frac{L'_{c_1}}{L_{c_n}} + 2^{n(N-1)}\xi'^2_m\,\frac{L_{c_{m_s}}}{L_{c_n}}\,\frac{L'_{c_{m_s}}}{L_{c_n}} + \sum_{\bar{2}}^{n}\left[2^{n-i(n-i+1)}\,\frac{L_{c_i}}{L_{c_n}}\,\frac{L'_{c_i}}{L_{c_n}}\right.\right.$$

$$\left.\left. + 2^{n-i+1(n-i+1)(N-1)}\,\frac{L_{c_{m_i}}}{L_{c_n}}\,\frac{L'_{c_{m_i}}}{L_{c_n}}\right]\right)$$

The reduced deflections result from the recurrence formulas:

$$\bar{f}_1 = \frac{1}{N}\Bigg\{4n\left(\frac{L_{c_1}}{L_{c_n}}\right)^2\left[\left(3\xi^2-3\xi+1\right)\frac{L'_{c_1}}{L_{c_n}}+2(N-1)\left(3\xi_m^2-3\xi_m+1\right)\frac{L'_{c_{m_s}}}{L_{c_n}}\right]$$

$$+1.644\,\frac{L'_{B_s}}{L_{c_n}}\,\frac{L_{c_s}}{L_{c_n}}\left[2n\left(\xi'^2-\xi'\xi'_m+\xi'^2_m\right)\frac{L_{c_s}}{L_{c_n}}+\frac{n-1}{2}\left(\xi'+\xi'_m\right)\right]+$$

$$+1.644(N-2)\,\frac{L'_{B_{m_1}}}{L_{c_n}}\,\frac{L_{c_s}}{L_{c_n}}\left(n\xi'^2_m\,\frac{L_{c_1}}{L_{c_n}}+\frac{n-1}{2}\,\xi'_m\right)$$

$$+4n\left(\frac{L_{c_s}}{L_{c_n}}\right)^2\left[\frac{1-\epsilon}{\epsilon}\,\xi^2\,\frac{L'_{c_1}}{L_{c_n}}+2(N-1)\,\frac{1-\epsilon_m}{\epsilon_m}\,\xi_m^2\,\frac{L'_{c_{m_s}}}{L_{c_n}}\right]\Bigg\} \quad \ldots\ldots\ldots (76)$$

$$\bar{f}_2 = \bar{f}_1+\frac{1}{N}\Bigg\{(n-1)\left(\frac{L_{c_2}}{L_{c_n}}\right)^2\left[\frac{L'_{c_2}}{L_{c_n}}+2(N-1)\,\frac{L'_{c_{m_2}}}{L_{c_n}}\right]$$

$$+0.822\,\frac{L_{c_2}}{L_{c_n}}\left[\frac{n\,\xi'+\xi'_m\,L_{c_s}+(n-1)\,L_{c_2}}{L_{c_n}}\,\frac{L'_{B_1}}{L_{c_n}}+(N-2)\,\frac{n\xi'_m L_{c_1}+\frac{n-1}{2}\,L_{c_2}}{L_{c_n}}\,\frac{L'_{B_{m_1}}}{L_{c_n}}\right]$$

$$+0.822\,\frac{L_{c_2}}{L_{c_n}}\,\frac{(n-1)L_{c_2}+(n-2)L_{c_3}}{L_{c_n}}\left(\frac{L'_{B_2}}{L_{c_n}}+\frac{N-2}{2}\,\frac{L'_{B_{m_2}}}{L_{c_n}}\right)\Bigg\} \quad \ldots\ldots\ldots (77)$$

. . .

$$\bar{f}_i = \bar{f}_{i-1}+\frac{1}{N}\Bigg\{(n-i+1)\left(\frac{L_{c_i}}{L_{c_n}}\right)^2\left[\frac{L'_{c_i}}{L_{c_n}}+2(N-1)\frac{L'_{c_{m_i}}}{L_{c_n}}\right]$$

$$+0.822\,\frac{L_{c_i}}{L_{c_n}}\left[\frac{(n-i+2)L_{c_{i-1}}+(n-i+1)L_{c_i}}{L_{c_n}}\,\frac{L'_{B_{i-1}}}{L_{c_n}}\right.$$

$$\left.+(N-2)\,\frac{\frac{n-i+2}{2}\,L_{c_{i-1}}+\frac{n-i+1}{2}\,L_{c_i}}{L_{c_n}}\,\frac{L'_{B_{m_{i-1}}}}{L_{c_n}}\right]$$

$$+0.822\,\frac{L_{c_i}}{L_{c_n}}\,\frac{(n-i+1)L_{c_i}+(n-i)L_{c_{i+1}}}{L_{c_n}}\left(\frac{L'_{B_i}}{L_{c_n}}+\frac{N-2}{2}\,\frac{L'_{B_{m_i}}}{L_{c_n}}\right)\Bigg\} \quad \ldots\ldots (78)$$

$$\bar{f}_n = \bar{f}_{n-1} + \frac{1}{N}\left\{1 + \frac{2(N-1)}{m_n} + 0{,}822\left(2\frac{L_{c_{n-1}}}{L_{c_n}} + 1\right)\left(\frac{L'_{B_{n-1}}}{L_{c_n}} + \frac{N-2}{2}\frac{L'_{Bm_{n-1}}}{L_{c_n}}\right) + 0.822\left(\frac{L'_{B_n}}{L_{c_n}} + \frac{N-2}{2}\frac{L'_{Bm_n}}{L_{c_n}}\right)\right\} \quad \ldots\ldots\ldots\ldots \quad (79)$$

Eqs. 67 and 68 may be used to compute the effective-length coefficients of the other columns.

Eqs. 60 through 79 have been obtained by an energetic method and contain all the principal parameters of the equilibrium-bifurcation problem. For the analysis of a pin-based frame it is sufficient to analyze its ground floor. For the fixed-base frame, similar formulas to these given previously, have been derived.

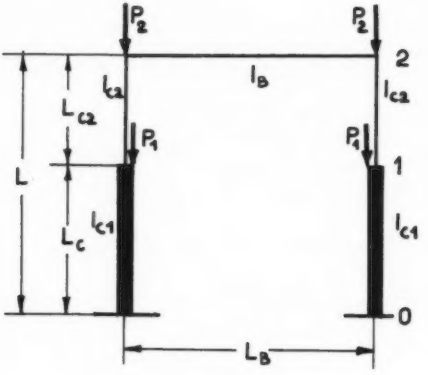

FIG. 16.—PORTAL FRAME WITH CRANE-LOADS.

Portal-Frame with Crane-Loads.—The stability equation of the symmetrical frame (Fig. 16) is

$$(1-\epsilon)\frac{\phi_1}{n\lambda}\left(a\frac{6\lambda}{\gamma} - b\phi_1\right) + 3\epsilon\left(\lambda\frac{6\lambda}{\gamma} + d\phi_1\right) = 0 \quad \ldots\ldots\ldots \quad (80)$$

in which:

$$a = 1 - \frac{1}{\sqrt{n(1-p)}}\tan\phi_1 \tan\phi_2 \; ; \qquad b = \tan\phi_1 + \sqrt{n(1-p)}\tan\phi_2 \; ;$$

$$c = \tan\phi_1 + \frac{1}{\sqrt{n(1-p)}}\tan\phi_2 \; ; \qquad d = 1 - \sqrt{n(1-p)}\tan\phi_1 \tan\phi_2 \, ,$$

with the notations

$$\lambda = \frac{L_{c_s}}{L_c} \; ; \quad \lambda' = \frac{L_{c_2}}{L_c} = 1 - \lambda \; ; \; n = \frac{E_{t_2} I_{c_2}}{E_{t_1} I_{c_s}} \; ; \; \gamma = \frac{E_{t_s} I_{c_s} L_B}{E_B I_B L_s} \; ; \; p = \frac{P_1}{P_s + P_2}$$

The approximate formulas

$$k_1 = \frac{R}{\lambda} \quad \ldots\ldots\ldots\ldots\ldots\ldots \quad (81)$$

$$k_2 = \frac{R}{\lambda'} \sqrt{\frac{n}{1-p}} \quad \ldots\ldots\ldots\ldots\ldots\ldots \quad (82)$$

and

$$R = \sqrt{2\mu \bar{f}_2 \; \frac{1 - p\left[1 - \frac{1}{\mu\lambda}\left(\frac{\bar{f}_1}{\bar{f}_2}\right)^2\right]}{1 - p\left(1 - \frac{\bar{f}_1}{\bar{f}_2}\right)}} \quad \ldots\ldots\ldots\ldots\ldots \quad (83)$$

may be used, with the reduced deflections

$$\bar{f}_1 = \lambda\left\{\lambda\,(2\lambda - 3\,\bar{m}_o) + 3\frac{\lambda'}{n}\,[2 - \lambda'\,(1+p) - 2\bar{m}_o] + \gamma'\,(1 - p\,\lambda' - \bar{m}_o)\right\} \ldots\ldots \quad (84)$$

and

$$\bar{f}_2 = \lambda^2(2\lambda - 3\,\bar{m}_o) + \frac{\lambda'}{n}\,[2(1+\lambda+\lambda^2) - p\lambda'\,(2+\lambda) - 3\,\bar{m}_o(1+\lambda)] + \gamma'\,(1 - p\lambda' - \bar{m}_o) \quad \ldots \quad (85)$$

with

$$\bar{m}_o = \frac{3}{2}\,\epsilon\,\frac{\lambda'[2 - \lambda'(1+p)] + \lambda^2 n + (1 - p\lambda')\frac{n\gamma'}{3}}{n\,\lambda + 3\,\epsilon\left(\lambda' + \frac{2}{3}\,n\,\lambda + \frac{n\gamma'}{6}\right)} \quad \ldots\ldots\ldots\ldots \quad (86)$$

The coefficient μ is obtained for

$$\xi \geq \lambda \text{ from } \mu = \frac{2}{n}\,\frac{(1-\xi)^2}{\bar{f}_{E_2}} \quad \ldots\ldots\ldots\ldots\ldots\ldots \quad (87)$$

$$\xi < \lambda \text{ from } \mu = \frac{1}{1+\lambda-2\xi}\left(1 + \frac{\bar{f}_{E_1}}{\bar{f}_{E_2}} - 2\frac{\bar{f}_{E_\xi}}{\bar{f}_{E_2}}\right) \quad \ldots\ldots\ldots\ldots \quad (88)$$

with

$$\xi = \frac{3}{2}\,\epsilon\,\frac{1 - \lambda^2(1-n)}{n\lambda + \epsilon\,(3\lambda' + 2n\lambda)} \;;\; \bar{f}_{E_2} = \lambda^2(2\lambda - 3\xi) + \frac{\lambda'}{n}\left[2(1+\lambda+\lambda^2) - 3(1+\lambda)\,\xi\right] \;;$$

$$\bar{f}_{E_1} = \lambda\left[\lambda\,(2\lambda - 3\xi) + \frac{3\lambda'}{n}\,(1+\lambda-2\xi)\right] \;;\; \bar{f}_{E_\xi} = \xi\left[2\xi^2 - 6\lambda\xi + 3\lambda^2 + \frac{3\lambda'}{n}\,(1+\lambda-2\xi)\right] .$$

Eqs. 81 through 88 resulted from an energetic analysis and may be particularized for pinned and fixed bases. Similar formulas have also been derived for frames with pinned connections between beam and columns, respectively for multi-bay frames, taking account of the non-symmetric loading. These computations also include (approximately) the spatial effect of the crane loading, in order to avoid an underestimation of the stability of the building.

The use of formulas of the type given previously, is only apparently more complicated than that of the known diagrams and charts, as these oversimplify the problem by elimination of some important parameters. The formulas could be compared to the well-known Kleinlogel formulas for the static-strength computation of frames, and to not assume special knowledge of the theory of stability on the designers part.

VARIOUS INSTABILITY MODES OF THE FIXED BASE COLUMN[a]

Discussion by James Chinn

JAMES CHINN,[4] M. ASCE.—The author has presented solutions to several cases of column buckling that are of considerable practical interest. Mr. Sawyer has rendered a valuable service to the profession through his paper.

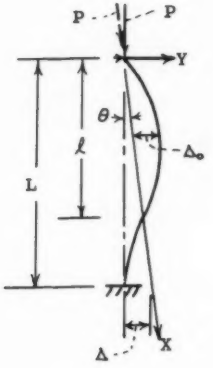

$$Y = \Delta_o \sin \frac{\pi X}{\ell} \; ; \quad Y' = \Delta_o \frac{\pi}{\ell} \cos \frac{\pi X}{\ell}$$

At X = L: $\quad -\Delta = \Delta_o \sin \frac{\pi L}{\ell}$

$$Y' = \tan \theta = -\frac{\Delta}{L} = \Delta_o \frac{\pi}{\ell} \cos \frac{\pi L}{\ell}$$

$$\frac{1}{L}\Delta_o \sin \frac{\pi L}{\ell} = \Delta_o \frac{\pi}{\ell} \cos \frac{\pi L}{\ell}$$

$$\tan \frac{\pi L}{\ell} = \frac{\pi L}{\ell} \qquad \text{but } \ell = \pi\sqrt{\frac{EI}{P}} = \frac{\pi}{k}$$

$$\tan \frac{\pi L}{\frac{\pi}{k}} = \frac{\pi L}{\frac{\pi}{k}}$$

$$\tan kL = kL$$

FIG. 15.—EXAMPLE 1

A less mathematical method that is applicable to the solution of prismatic columns was presented by Haarman[5] and is taught at Cornell University (Ithaca, N. Y.) by George Winter and Paul P. Bijlaard, Fellows, ASCE. The writer has applied this method in Figs. 15 through 18 to the problems solved by the author.

---

[a] July 1960, by D. A. Sawyer (Proc. paper 2544).

[4] Prof. of Civ. Engrg., Univ. of Colorado, Boulder, Colo.

[5] "Geometerical Location of Inflection Points," by Haarman, (In Dutch), pp. 1918-26.

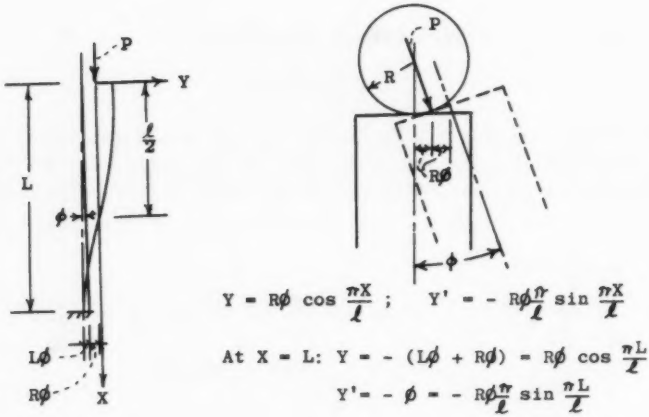

$$Y = R\phi \cos \frac{\pi X}{\ell} \; ; \quad Y' = - R\phi \frac{\pi}{\ell} \sin \frac{\pi X}{\ell}$$

At X = L: $Y = - (L\phi + R\phi) = R\phi \cos \frac{\pi L}{\ell}$

$$Y' = - \phi = - R\phi \frac{\pi}{\ell} \sin \frac{\pi L}{\ell}$$

$$\cos \frac{\pi L}{\ell} = - \left(1 + \frac{L}{R}\right) ; \quad \sin \frac{\pi L}{\ell} = \frac{\ell}{R\pi}$$

$$\tan \frac{\pi L}{\ell} = - \frac{\frac{\ell}{R\pi}}{1 + \frac{L}{R}} \quad \text{but } R = mL$$

$$= - \frac{\frac{\ell}{\pi mL}}{1 + \frac{L}{mL}} = - \frac{\frac{\ell m}{\pi mL}}{m + 1} = - \frac{\frac{\ell}{\pi L}}{m + 1}$$

but $\ell = \frac{\pi}{k}$

$$\tan \frac{\pi Lk}{\pi} = - \frac{\frac{\pi}{\pi kL}}{m + 1}$$

$$\tan kL = - \frac{1}{kL(m + 1)}$$

FIG. 16.—EXAMPLE 2

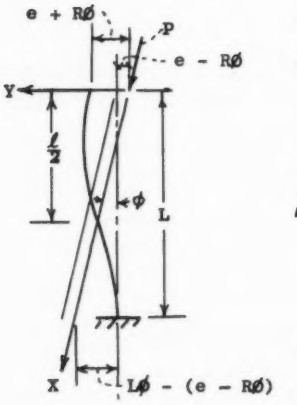

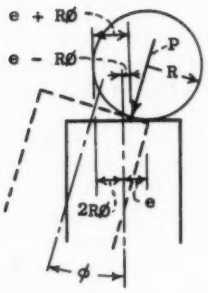

$$Y = (e + R\emptyset)\cos\frac{\pi X}{\ell}\ ;\ Y' = -\frac{\pi}{\ell}(e + R\emptyset)\sin\frac{\pi X}{\ell}$$

At $X = L$: $Y = -\left[L\emptyset - (e - R\emptyset)\right]$

$$= (e + R\emptyset)\cos\frac{\pi L}{\ell}$$

$$Y' = -\emptyset = -\frac{\pi}{\ell}(e + R\emptyset)\sin\frac{\pi L}{\ell}$$

$$\cos\frac{\pi L}{\ell} = -\frac{L\emptyset - e + R\emptyset}{R\emptyset + e} \qquad \sin\frac{\pi L}{\ell} = \frac{\ell}{\pi}\frac{\emptyset}{e + R\emptyset}$$

$$= -\frac{L - \frac{e}{\emptyset} + R}{R + \frac{e}{\emptyset}} \qquad = \frac{\ell}{\pi}\frac{1}{\frac{e}{\emptyset} + R}$$

$$\tan kL = -\frac{\frac{\ell}{\pi}\frac{1}{R + \frac{e}{\emptyset}}}{\frac{L - \frac{e}{\emptyset} + R}{R + \frac{e}{\emptyset}}} = -\frac{\frac{\ell}{\pi}}{L - \frac{e}{\emptyset} + R} = -\frac{\frac{1}{k}}{L - \frac{e}{\emptyset} + R}$$

$$L - \frac{e}{\emptyset} + R = -\frac{1}{k\tan kL}\ ;\ \frac{e}{\emptyset} = \frac{1}{k\tan kL} + L + R = \frac{1 + (L + R)k\tan kL}{k\tan kL}$$

$$\emptyset = \frac{ke\tan kL}{1 + (L + R)k\tan kL} = \frac{ke\tan kL}{kL(m + 1)(\tan kL) + 1}$$

FIG. 17.--EXAMPLE 3

Haarman's method is based on recognizing that the elastic curve of a prismatic column or beam-column is made up of portions of sine waves between points of load application. The equation of the curve is

$$y = \Delta_o \sin \frac{\pi x}{l} \quad \ldots\ldots\ldots\ldots\ldots\ldots \quad (58a)$$

or

$$y = \Delta_o \cos \frac{\pi x}{l} \quad \ldots\ldots\ldots\ldots\ldots\ldots \quad (58b)$$

depending on the choice of origin; y is the ordinate of a point on the elastic curve measured laterally from the line of action of the resultant force, x represents the distance from origin to point measured along the line of action, Δ_o is the amplitude of the sine wave, and l denotes the length of the half-sine wave. The load on the column is related to l through the Euler formula,

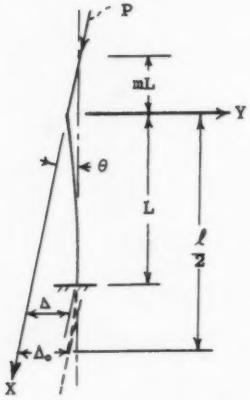

$$Y = \Delta_o \sin \frac{\pi X}{\ell} \; ; \qquad Y' = \Delta_o \frac{\pi}{\ell} \cos \frac{\pi X}{\ell}$$

At X = L: $\Delta = \Delta_o \sin \frac{\pi L}{\ell}$

$$Y' = \tan \theta = \frac{\Delta}{L + mL}$$

$$= \Delta_o \frac{\pi}{\ell} \cos \frac{\pi L}{\ell}$$

$$\Delta_o \frac{\pi}{\ell} \cos \frac{\pi L}{\ell} = \Delta_o \sin \frac{\pi L}{\ell} \; \frac{1}{L(1 + m)}$$

$$\tan \frac{\pi L}{\ell} = \frac{\pi L(1 + m)}{\ell}$$

but $\ell = \pi \sqrt{\frac{EI}{P}} = \frac{\pi}{k}$

$$\tan kL = kL(1 + m)$$

FIG. 18.—EXAMPLE 4

$$P = \frac{\pi^2 E I}{l^2} \quad \ldots\ldots\ldots\ldots\ldots\ldots \quad (59)$$

and

$$l = \pi \sqrt{\frac{E I}{P}} = \frac{\pi}{k} \quad \ldots\ldots\ldots\ldots\ldots\ldots \quad (60)$$

in which $k = \sqrt{\frac{P}{E I}}$.

METHOD FOR ANALYSIS OF MULTIBEAM BRIDGES[a]

Discussion by A. S. Arya

A. S. ARYA,[4] A. M. ASCE.—Different approaches have been used by various authors for the study of load distribution in floor beams and stringers in highway bridges.

For analyzing grid-type decks, A. J. S. Pippard, F. ASCE and J. P. A. De Waele developed[5] a method in which the total stiffness of transverse beams was distributed uniformly over the length of the bridge and obtained their solution in the form of fourth-order simultaneous ordinary differential equations. M. Hetenyi, F. ASCE used the same approach but expressed the concentrated loads in terms of Fourier series that resulted in algebraic simultaneous equations for each term of the series instead of simultaneous differential equations.[6] The authors' approach for analyzing multibeam-type bridges is similar to Hetenyi's, with the difference that the connection between the elements cannot transfer moment and can transfer shearing stresses only. The paper, however, has great merit in that it includes the effects of torsional stiffness and torsion-bending characteristics of the beam elements.

The other approach is that of orthotropic plate theory used by Y. Guyon,[7] C. Massonet,[8] P. B. Morris and G. Little[9] and others. In this approach a question arises about the stiffnesses of the slab, especially the transverse flexural and torsional stiffnesses. Apparently these would be greatly influenced by the magnitude of transverse prestress. The results obtained[10] by R. Walther indicate that the maximum proportion of the load that goes to any element is

---

[a] July 1960, by John E. Duberg, Narbey Khachaturian, and Raul E. Fradinger (Proc. paper 2552).

[4] Reader in Civ. Engrg., Univ. of Roorkee, U. P., India; presently, Doctorate Student at the Univ. of Illinois, Urbana, Ill.

[5] "The Loading of Interconnected Bridge Girders," by A. J. S. Pippard and J. P. A. De Waele, Journal, I. C. E., London, Vol. 10, 1938, pp. 97-114.

[6] "A Method for Calculating Grillage Beams," by M. Hetenyi, S. Timoshenko 60th Annual Vol., New York, 1938, pp. 60-72.

[7] "Calcul des Ponts Larges à Poutres Multiples Solidarisées par des Entretoises," by Y. Guyon, Annales des Ponts et Chausees, No. 24, Septembre, Octobre, 1946, pp. 553-612.

[8] "Méthod de Calcul des Ponts à Poutres Multiples Tenant Compte de Leur Résistance à la Torsion," by C. Massonet, I. A. B. S. E., Vol. 10, Zurich, 1950, pp. 147-182.

[9] "Load Distribution in Prestressed Concrete Bridge Systems," by P. B. Morris and G. Little, The Structural Engineer, Vol. 32, No. 3, March, 1954, pp. 83-111.

[10] "Investigation of Multibeam Bridges," by R. Walther, Journal, ACI, December, 1957, pp. 505-526.

largely influenced by the ratio of transverse prestressing force to the load on the bridge. According to his results, an increase in the ratio of the transverse prestressing force to the acting load results in a decrease in the moment that goes to the most heavily loaded element. The authors' assumption of hinged joints between the elements is, therefore, a conservative one and is justified by the absence of definite specifications regarding the magnitude of the transverse prestressing force. To study the effect of transverse stiffness at joints one may replace the longitudinal hinges of the authors by spirals having the twisting stiffness K such that if there is a rotation θ at the joint, a moment $K\theta$ is produced at it. The stiffness K will be an empirical property to be determined by tests. This would, of course, complicate the equations. Yet the superiority of the method, in the writer's belief, is that the structure analyzed does not become something different from the actual; on the contrary it retains all its properties almost as such and can be used as a practical method for obtaining solutions on a digital computer.

For obtaining numerical solutions, Eqs. 46, 47, and 48 can be expressed in the following form:

$$-\left[\frac{2(p_j - p_{j+1})}{n^2\pi^2 k} + \frac{(p_j \epsilon_j + p_{j+1}\epsilon_{j+1})\beta^2}{k R \beta^2 n^2(\pi^2+1)}\right] \sin\frac{n\pi c}{L}$$

$$= -\frac{\bar{z}/b}{n\pi k}\left[q_{(j-1)n} - 2q_{jn} + q_{(j+1)n}\right] - \frac{\beta\,\bar{z}/b}{2(k R \beta^2 n^2(\pi^2+1)}\left[r_{(j-1)n} - r_{(j+1)n}\right]$$

$$-\frac{1}{n^2\pi^2 k\beta}\left[s_{(j-1)n} - 2s_{jn} + s_{(j+1)n}\right]$$

$$+\frac{\beta}{4(kR\beta^2 n^2\pi^2+1)}\left[s_{(j-1)n} + 2s_{jn} + s_{(j+1)n}\right] \ldots\ldots\ldots\ldots (79)$$

$$-\frac{2(p_j \epsilon_j - p_{j+1}\epsilon_{j+1})\beta^2 \bar{z}/b}{k R \beta^2 n^2 \pi^2 + 1} \sin\frac{n\pi c}{L}$$

$$= -\frac{i}{2n\pi k}\left[q_{(j-1)n} - q_{(j+1)n}\right] - \left(\frac{i}{n^2\pi^2 k\beta} + \frac{\beta(\bar{z}/b)^2}{kR\beta^2 n^2\pi^2+1}\right)\left[r_{(j-1)n}\right.$$

$$\left. -2r_{jn} + r_{(j+1)n}\right] + \frac{\beta\,\bar{z}/b}{2(kR\beta^2 n^2\pi^2+1)}\left[s_{(j-1)n} - s_{(j+1)n}\right] \ldots\ldots\ldots (80)$$

and

$$-\left[\frac{2(p_j-p_{j+1})\,\beta\bar{z}/b}{n^2\pi^2 k}+\frac{2(p_j\,\epsilon_j+p_{j+1}\,\epsilon_{j+1})\,\beta^3 Q}{k R \beta^2 n^2\pi^2+1}\right]\sin\frac{n\pi c}{L}$$

$$=-\frac{\beta}{n\pi k}\left(\frac{i}{a}+\left(\frac{\bar{z}}{b}\right)^2-\frac{i}{4}\right)\left[q_{(j-1)n}+q_{(j+1)n}\right]$$

$$+\frac{2\beta}{n\pi k}\left[\frac{i}{a}+(\bar{z}/b)^2+\frac{i}{4}\right]q_{jn}$$

$$+\left(\frac{i}{2n^2\pi^2 k}-\frac{\beta^2 Q\,\bar{z}/b}{k R\beta^2 n^2\pi^2+1}\right)\left[r_{(j-1)n}-r_{(j+1)n}\right]$$

$$-\left(\frac{\bar{z}/b}{n^2\pi^2 k}-\frac{\beta^2 Q}{2(kR\beta^2 n^2\pi^2+1)}\right)\left[s_{(j-1)n}+s_{(j+1)n}\right]$$

$$+\left(\frac{2\,\bar{z}/b}{n^2\pi^2 k}+\frac{\beta^2 Q}{k R\beta^2 n^2\pi^2+1}\right)s_{jn} \quad \ldots\ldots\ldots\ldots\ldots\ldots \quad (81)$$

where $k = E I_{xy}/(G J)$, $i = I_{xy}/I_{zx}$, $a = A b^2/I_{zx}$, $\beta = b/L$, $\epsilon = e/b$, $Q = \bar{\Omega}/b^2$, $R = C/I_{xy} b^2$, and $p_j = P_j/b$. All other terms are defined in the text of the paper. From Eqs. 79, 80, and 81, it follows that the solution of the problem depends on eight dimensionless parameters. To obtain general solutions based on all the eight parameters appears to be a colossal task at first sight especially when the sets of simultaneous equations are to be solved for different values of n. However, from purely physical considerations it appears that the parameter k involving the flexural rigidity $E I_{xy}$ and torsional rigidity $G J$ is likely to be the most significant quantity so far as M_{xy} in any element is concerned. Furthermore, a study by the writer has shown that for a particular shape the other parameters can be approximately expressed in terms of one or two parameters only, so that the number of independent variables can be greatly reduced. For example, it was found that for closed sections similar to the Standard BPR slab and box sections, all other parameters can be expressed in terms of k within an accuracy of 10%. For open sections, such as channel sections, an additional independent variable i is needed, because the variation of the thickness of the legs is found to have an appreciable effect on some properties. It therefore follows that the shape of the section is a major variable and for a given shape just one or two parameters are sufficient to define the problem.

In order to obtain the geometric properties of sections, namely, A, I_{xy}, I_{xz}, J, $\bar{z}$, $\bar{\Omega}$, and C the gross concrete area may be considered. Therefore A, I_{xy}, and I_{xz} may be computed as usual; the determination of J, $\bar{z}$, $\bar{\Omega}$ and C is briefly discussed in the following paragraphs.

Determination of J.

(a) Box-Sections.—Using the membrane theory, and taking H as the height of the membrane, torque T on the section is twice the volume under membrane (Fig. 8):

$$T \doteq 2(b - t_1)(h - t_2)H \quad \ldots\ldots\ldots\ldots\ldots\ldots (82)$$

Also

$$\int \tau \, dt = 2 G \theta A \quad \ldots\ldots\ldots\ldots\ldots\ldots (83)$$

in which τ is the shear stress along any chosen core, for example ABCD, and A is the area of the core. Hence,

$$\left[\frac{H}{t_1} 2(h - t_2) + \frac{H}{t_2} 2(b - t_1)\right] = 2 G \theta (b - t_1)(h - t_2) \quad \ldots\ldots\ldots (84)$$

and

$$T = J G \theta \quad \ldots\ldots\ldots\ldots\ldots\ldots\ldots (85)$$

From Eqs. 82, 84, and 85

$$J = \frac{2 t_1 t_2 b^2 h^2 (1 - t_1/b)^2 (1 - t_2/h)^2}{b t_1 + h t_2 - (t_1^2 + t_2^2)} \quad \ldots\ldots\ldots\ldots (86)$$

Eq. 86 is a rational, though approximate, expression for J. Another approach can be used for computing J for box sections. This is to take the difference of J-values for the outside and inside rectangles. The value of J or a rectangle is given by St. Venant's expression

$$J = k_1 b h^3 \quad \ldots\ldots\ldots\ldots\ldots\ldots (87)$$

in which $b > h$, and k_1 varies with b/h, values of which are:[11]

b/h	1.0	1.5	2.0	2.5	3.0	4.0	10.0	∞
k_1	0.141	0.196	0.229	0.249	0.263	0.281	0.312	1/3

Furthermore, to have a check on the suitability of either of these methods, a section having the dimensions b = 48 in., h = 27 in., $t_1 = t_2 = 6$ in. has been analyzed by a finite-difference procedure using the following differential equation of torsion

$$\frac{\partial^2 \phi}{\partial x^2} + \frac{\partial^2 \phi}{\partial y^2} = -2 G \theta \quad \ldots\ldots\ldots\ldots\ldots (88)$$

Spacing the nodal points 3 in. apart and using Simpson's rule, the volume under the ϕ-surface results in T/2. Taking this as 'exact' the following shows a comparison between J obtained by the three methods:

Exact	1920×3^4 in.^{4}	100%
Membrane	1830×3^4 in.^{4}	95.4%
Difference of Rectangles	2128×3^4 in.^{4}	111%

11 "Theory of Elasticity," by S. Timoshenko and J. N. Goodier, McGraw-Hill Pub. Co., Inc., New York, 1951, p. 277.

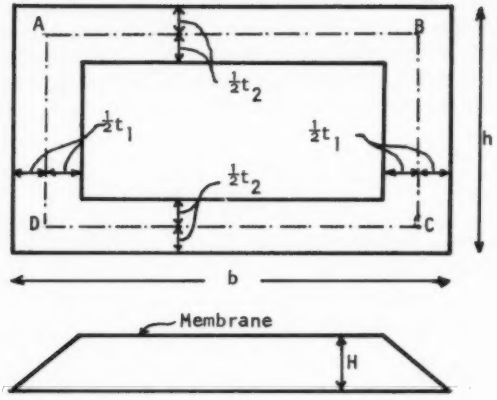

FIG. 8

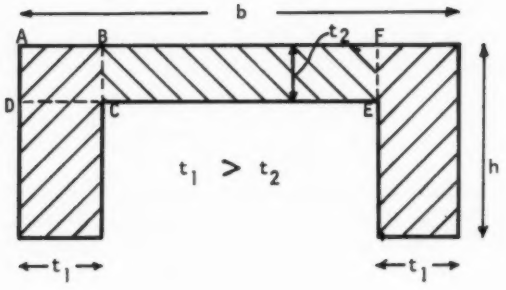

FIG. 9

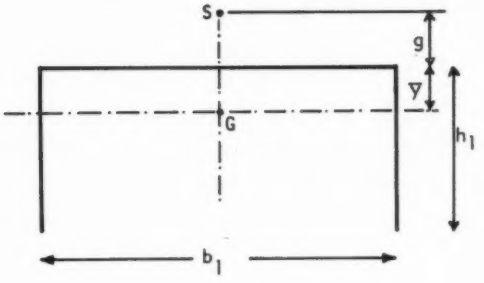

FIG. 10

This demonstrates the suitability of Eq. 86 for computing J for box sections. It is expected that the error will be even smaller for sections having smaller t/h and t/b ratios. On the other hand, the error in the "Difference method" is expected to become smaller for increasing ratios of t/b and t/h, becoming zero when the section becomes solid.

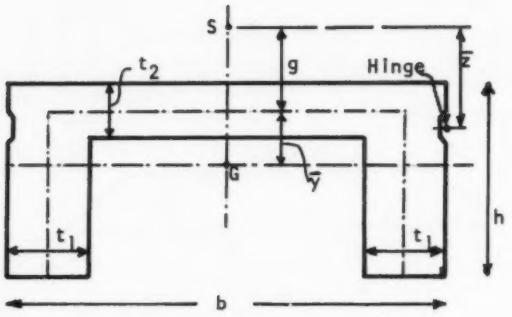

FIG. 11

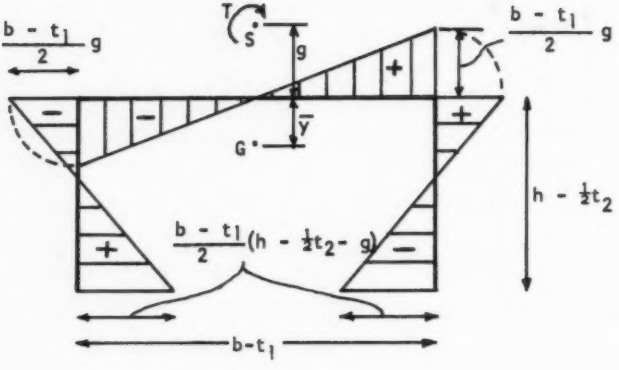

FIG. 12

(b) Slab-Sections.—Slab-sections presently in use are either solid or have circular holes. Based on the foregoing discussion the following formulas can be used:

Solid $$J = K_1 b h^3 \quad \ldots\ldots\ldots\ldots\ldots\ldots \quad (89)$$

With Holes $$J = K_1 b h^3 - \Sigma \frac{\pi}{32} d^4 \quad \ldots\ldots\ldots\ldots\ldots \quad (90)$$

in which d is the diameter of hole.

(c) Channel-Sections.—Using the concepts of membrane analogy the area of the channel may be divided into 3 rectangles shown shaded in Fig. 9. The area of the corner is taken with t_1 because $t_1 > t_2$. Now the rectangle BCEF has approximately the same conditions at its ends BC and EF as a portion of an infinitely long member. Consequently, the following formula may be used to compute J:

$$J = 2\, k_1\, h\, t_1^3 + \frac{1}{3}\,(b - 2\,t_1)\,t_2^3 \quad \ldots\ldots\ldots\ldots\ldots (91)$$

Again to check the accuracy of this expression a section with b = 45 in., h = 18 in., t_1 = 9 in., t_2 = 6 in. has been analyzed by the finite-difference procedure, taking the pivotal points 3 in. apart. The following is the comparison between the two values:

Exact	99.7×3^4 in.^{4}	100%
Membrane	98.2×3^4 in.^{4}	98.5%

Determination of $\bar{z}$.—The quantity $\bar{z}$ indicates the position of the hinge that is measured from the shear center of the section. The authors seem to have preferred to locate the hinge at the top corners of the section. In fact the shear keys are located below the top fiber and consist of a finite depth. The writer would prefer to assume the hinge at the center of the shear key. By symmetry the shear center of slab and box sections coincides with their center of gravity. For thin channels as shown in Fig. 10 the shear center S is located by finding g given by

$$g = \frac{A\,\bar{y}\,b_1^2}{4\,I_{zx}} \quad \ldots\ldots\ldots\ldots\ldots\ldots (92)$$

The writer believes that Eq. 92 may be used although the channels are not thin. The center-line dimensions can be used for b and h. For an actual channel the dimensions $\bar{y}$, g, etc. would be as shown in Fig. 11 and the formula will become

$$g = \frac{A\,\bar{y}\,(b - t_1)^2}{4\,I_{zx}} \quad \ldots\ldots\ldots\ldots\ldots\ldots (93)$$

Determination of $\bar{\Omega}$ *and* C.—The quantities Ω and C are believed to be small for slab and box sections in comparison to the other properties and can be taken as zero. They may however, be of some significance in the case of open sections like channels and should, therefore, be computed. Assuming a thin section and using the notation of Fig. 11, C may be expressed as

$$C = \frac{I_{xy}\,(b - t_1)^2}{4}\left[1 - \frac{A\,\bar{y}\,(g - \bar{y})}{I_{xy}}\right] \quad \ldots\ldots\ldots\ldots (94)$$

The distribution of unit warping Ω at the center line of the section is shown in Fig. 12. From Fig. 12 the unit warping at the level of the hinge $\bar{\Omega}$ may be easily found.

The error due to the assumption of a thin section is not certain and the writer would like to know if the authors considered this aspect of the problem and what their findings were.

A. R. ROBINSON,[12] A. M. ASCE.--The authors have presented a useful analytical study that serves to determine the distribution of loads among the beams of a multibeam bridge. In view of the usual method of attaching the beams it may be desirable to modify the authors' theory, to include the effect of transverse stiffness. Such transverse flexural stiffness should increase the uniformity of load distribution still further.

One apparent difficulty in extending the theory expounded by the authors is the contradiction between transverse bending and the engineering theory of flexure and torsion of beams used in the paper. The engineering theory makes use of the assumption that a cross section of the beam does not distort in its own plane; transverse bending, however, constitutes just such a distortion. A way of avoiding this difficulty is to lump the transverse flexibility at the "hinges" that connect the beams. According to this scheme of lumped flexibility, moments are exerted by the hinges on the adjacent beams proportional to the relative rotation of these beams. A hinge may be imagined to contain springs that resist relative rotation of the two parts of the hinge.

The modifications required in the theory are not extensive. First, the free-body diagram of a general beam element must be altered to include the moments exerted by the joints on the beams. The joint between the j^{th} and $(j+1)^{th}$ beam exerts the moment $m_j\,dx$ on an element of the j^{th} beam, with positive direction indicated by Fig. 13.

The "running" moments m_j can be expressed in terms of ϕ_j and ϕ_{j+1} as

$$m_j = K(\phi_{j+1} - \phi_j) \quad \ldots\ldots\ldots\ldots\ldots\ldots \quad (95)$$

in which K is the effective rotational spring constant of the elastic joints (in units of force, because m_j is a moment per unit length). The presence of m_j and m_{j-1} on beam j affects only one of the six equations of equilibrium of an element, namely, the sum of moments about the x-axis:

$$\sum M_x = 0:$$

$$M_{jx} + dM_{jx} - M_{jx} + (s_j + s_{j-1})\frac{b}{2}\,dx + (r_j - r_{j-1})\,\bar{z}\,dx + e\,dP_j + (m_j - m_{j-1})\,dx = 0 \quad \ldots\ldots\ldots\ldots \quad (96)$$

or

$$\frac{dM_{jx}}{dx} = t_j = -(s_j + s_{j-1})\frac{b}{2} - (r_j - r_{j-1})\,\bar{z} - \frac{dP_j}{dx}\,e - (m_j - m_{j-1}) \quad \ldots \quad (97)$$

Substituting Eq. 95 into Eq. 97 and expressing t_j in terms of ϕ_j as in Eq. 3 of the paper, we have

$$-E\,C\frac{d^4\phi_j}{dx^4} + G\,J\frac{d^2\phi_j}{dx^4} - 2\,K\,\phi_j = -\left(s_j + s_{j-1}\frac{b}{2}\right) - (r_j - r_{j-1})\,\bar{z} - \frac{dP_j}{dx}\,e - K(\phi_{j-1} + \phi_{j+1}) \quad \ldots\ldots\ldots\ldots\ldots \quad (98)$$

Eq. 98 now replaces the sum of Eqs. 11 and 23. Of course, P_j may still be expanded into a Fourier Series in the same way as was done previously. All other equations of equilibrium remain unaltered, as do the three continuity equations (Eqs. 43, 44, and 45). Examination of Eq. 98 shows immediately that the series expressions for q_j, r_j, and s_j (Eqs. 25, 26, and 27), are still consistent with a

---

[12] Assoc. Prof. of Civ. Engrg., Univ. of Illinois, Urbana, Ill.

sine Fourier series for the ϕ_j's. However, the presence of the terms ϕ_{j-1} and ϕ_{j+1} in Eqs. 98 no longer allows the simple expression, Eq. 41, for the Fourier coefficients of ϕ_j in terms of those of q_i, r_i, and s_i. The computational

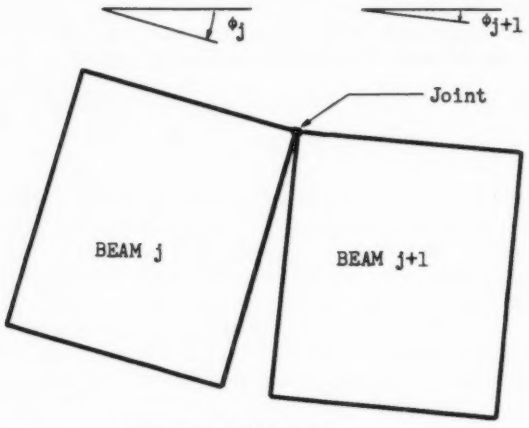

ANGLES OF ROTATION
(SHOWN POSITIVE WHEN VIEWED FROM
THE POSITIVE END OF THE x - AXIS)

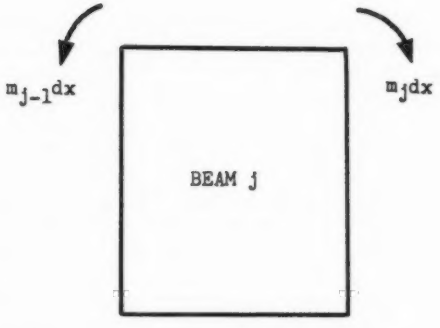

ADDITIONAL MOMENTS EXERTED ON AN ELEMENT OF THE jth BEAM
(SEEN FROM THE POSITIVE END OF THE x - AXIS)

FIG. 13

scheme for finding the Fourier coefficients for the moments and shears must then be changed. One way of doing this is to express u_j, v_j, and w_j in the continuity equations, as before, in terms of the constraining forces q, r, and s,

leaving ϕ_j in these equations. To this set of equations those of form of Eq. 98 are appended to form a set of 4 m+1 equations in 4 m+1 unknowns, m being the number of joints. Previously there were just 3 m equations in 3 m unknowns for each term of the Fourier series.

Determination of the exact value of K may present some difficulty. Perhaps all one requires are upper and lower bounds on K to learn whether or not the effect of transverse stiffness is important in specific cases.

BASIC COLUMN STRENGTH[a]

Discussion by John W. Fisher and Ivan M. Viest

JOHN W. FISHER,[19] A. M. ASCE, and IVAN M. VIEST,[20] F. ASCE.—Although the yield point is a property basic to the design of steel structures, the information available to structural engineers on the effects of testing speed and of residual stresses on the yield point is limited. The number of tests reported by the authors is large; however, even further extensive and systematic studies are needed to determine the variation in these effects.

A comprehensive series of static tests of structural steel and several residual stress studies have been conducted in connection with tests of bridges at the AASHO Road Test, a research project sponsored by the American Association of State Highway Officials and administered by the Highway Research Board of the National Academy of Sciences-National Research Council. The results are presented as a supplement to the information reported by the authors.

Mechanical Properties.—The results of ninety-eight static tension tests concerning the yield-stress level are reported in Table 3. The tests were carried out in a 100,000-lb capacity screw-type mechanical testing machine. The data presented in Table 3 covered six different heats, five sizes of rolled wide-flange beams, and one thickness of plate material.

The order of testing the coupons was randomized with respect to heat and thickness. The testing procedure was comparable to that reported by the authors. The load was applied at a rate of 140 μ in./in. sec up to the yielding of the steel. The yield point was determined by the drop-of-beam of the testing machine. No significant difference was found to exist between the drop-of-beam yield and the yield stress level (σ_y) for the speed of testing used. This same rate of straining was continued in the plastic region up to the point of strain hardening; however, in the plastic region the testing machine was stopped three times and few minutes were allowed to elapse to enable the load to decrease to the minimum value and thus to determine the value of the static yield point (The mean of the three minimum values was taken as the static yield point). Deformations were observed on each specimen with an 8-in. extensometer up to strain hardening to assure that the static level was approached through increasing rather than decreasing strain.

One hundred fourty-four tests were carried out on material from heats 90, 74, 83, and 42. However, the static yield points were not obtained during these tests. The mean drop-of-beam yield and ultimate strength for the four heats

---

[a] July 1960, by Lynn S. Beedle and Lambert Tall (Proc. paper 2555).

[19] Asst. Bridge Research Engr., Highway Research Bd., AASHO Road Test, Ottawa, Ill.

[20] Bridge Research Engr., Highway Research Bd., AASHO Road Test, Ottawa, Ill.

was in no case different at the 5% level of significance from the means of the corresponding heats reported herein.

Mean values and standard deviations are shown in Table 3 for the static yield point and the drop-of-beam yield point of each heat. For each type of measurement, including the static yield point, the drop-of-beam yield point, the ultimate strength, and the modulus of elasticity, an analysis of variance was made to determine the variation between specimens within a heat, and between heats. At the 5% level of significance, there was no difference in the static yield point, drop-of-beam yield point, or the ultimate strength between specimens of the same thickness and from the same heat. However, the dif-

TABLE 3.—YIELD POINT OF COUPONS FROM WIDE FLANGE BEAMS AND COVER PLATES

Heat	Beam Size	Number of Beams or Plates	Static Yield Point			Drop-of-Beam Yield Point			Mill Test
			Number of Specimens	σ_{ys}, in ksi	s*, in ksi	Number of Specimens	σ_y, in ksi	s, in ksi	σ_y, in ksi
(1)	(2)	(3)	(4)	(5)	(6)	(7)	(8)	(9)	(10)
FLANGE SPECIMENS									
90	18 WF 50	3	6	35.9	1.98	6	38.8	2.24	
74	18 WF 55	3	6	31.5	1.22	6	34.4	1.15	
83	21 WF 62	2	4	32.1	1.08	4	34.9	1.24	
42	18 WF 60	5	10	32.8	1.55	10	35.5	1.62	
36	18 WF 96	6	24	29.9	1.04	24	32.5	1.21	
WEB SPECIMENS									
90	18 WF 50	3	3	36.8	4.08	3	39.8	4.22	38.2
74	18 WF 55	3	3	36.6	1.27	3	39.5	1.22	40.3
83	21 WF 62	2	2	37.3	0.95	2	39.8	1.36	41.3
42	18 WF 60	5	5	36.8	1.79	5	39.6	1.60	39.9
36	18 WF 96	6	11	33.2	1.09	11	36.0	1.09	37.9
PLATE									
85	7/16 x 6 12	12	24	34.8	1.02	24	37.4	1.04	36.1

*s = standard deviation.

ference between heats was usually significant. No significant difference between any specimens was found for the modulus of elasticity.

The large number of corresponding data on the static yield point and the drop-of-beam yield point makes possible a statistical analysis of the effect of heat, thickness, and yield-stress level on the ratio of the dynamic yield stress to the static yield stress for the strain rate of 140 μ in./in. sec. Tests at the 5% level of significance indicated no effect of heat, thickness, or yield-stress level on the ratio of dynamic yield stress to the static yield stress. Hence, the mean value of the ratio, 1.08, represents all tests reported herein regardless of the source.

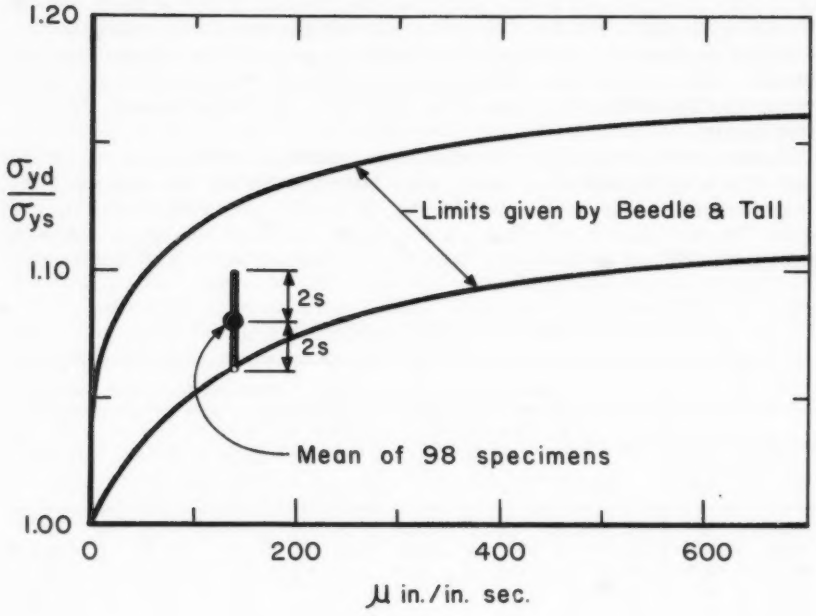

FIG. 35.—INFLUENCE OF STRAIN RATE ON YIELD STRESS LEVEL

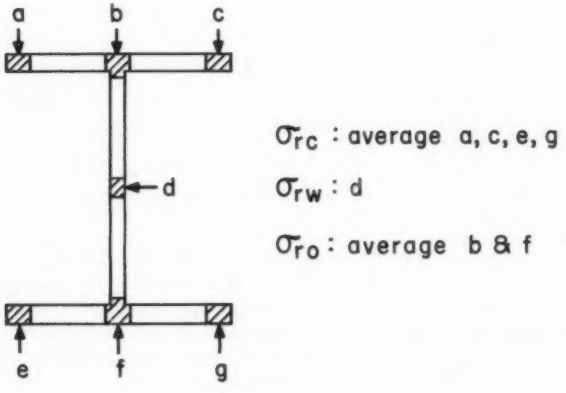

FIG. 36.—LOCATION OF RESIDUAL STRESS MEASUREMENTS

The mean ratio of dynamic to static yield stress is compared in Fig. 35 with the limits suggested by the authors. The spread of the writers' data is indicated by the 95% confidence limits (95% confidence limits correspond to $\pm$ 2 s around the mean). The mean falls within the range of the authors' data but is located closer to the lower than to the upper limit. Furthermore, the range between the 95% confidence limits is narrower than the range between the suggested limits.

Residual Stress.—Residual stresses were determined from sixteen wide-flange beams by the method of sectioning. Measurements were made on a 10-in. gage length at locations shown in Fig. 36 on six 9-ft beams and ten 2-ft beams. The 9-ft beams had first a 2-ft section cut out of the center that was then cut into strips $\frac{1}{2}$ in. wide and 11 in. long. Readings were taken before cutting, after the 2-ft section was cut out, and again after the 2-ft section was cut into strips. The 2-ft beams were sectioned into strips $\frac{1}{2}$ in. x 11 in. after initial readings were taken; a second set of readings was taken on the strips.

TABLE 4.—RESIDUAL STRESSES

Test No. (1)	Heat (2)	Shape (3)	Obtained from 9-ft Beams: σ_{rc}, in ksi (4)	σ_{rc}, in ksi (5)	σ_{rw}, in ksi (6)	Obtained from 2-ft Beams: σ_{rc}, in ksi (7)	σ_{ro}, in ksi (8)	σ_{rw}, in ksi (9)
9A1	36	18 WF 96	- 6.7	-9.5	15.8	-1.9	-7.6	0.9
9A2	36	18 WF 96	- 9.5	-6.4	12.4	-4.4	-4.1	9.5
9A3	36	18 WF 96	- 9.9	0.2	6.8	-8.7	0.7	5.5
9B1	36	18 WF 96	-11.1	-2.9	10.7	-7.3	-1.4	9.2
9B2	36	18 WF 96	-13.5	-7.9	9.6	-8.7	-5.4	6.9
9B3	36	18 WF 96	-13.3	-7.0	13.5	-7.4	-5.2	8.5
1A1	74	18 WF 55				-6.1	16.9	-16.1
1A2	74	18 WF 55				-6.4	16.5	-17.2
1B1	90	18 WF 50				-8.8	11.9	-13.6
2B1	90	18 WF 50				-9.5	17.8	-10.8
3A1	93	21 WF 62				-8.3	13.7	- 7.3
3A2	83	21 WF 62				-9.8	17.5	- 8.9
3A3	83	21 WF 62				-7.2	15.3	- 8.3
3B3	42	18 WF 60				-9.4	14.7	-13.0
4A2	42	18 WF 60				-4.7	7.2	- 9.2
4B1	86	18 WF 60				-1.4	1.0	-15.4

The results obtained from the 2-ft specimens do not represent the residual stresses present in longer beams. However, they allow a study of the variation between beams within a heat and between heats.

Table 4 contains a listing of all specimens by heat and shape. The residual stresses for 9-ft beams are based on the difference in measurements made on these beams and those made after the beams were cut into strips. The residual stresses listed for 2-ft beams is the difference between measurements made before and after the 2-ft beams were cut into strips. The residual stress at the flange edge (σ_{rc}) listed in Table 4 is the average for the four flange

tips. The residual stress listed as the flange center (σ_{ro}) is the average of the two flange center measurements.

The residual stresses obtained from the 9-ft 18WF96 beams can be compared to those presented by the authors. The ratio of the depth of section to its flange width, d/b, for the 18WF96 beam is 1.55, making it a borderline case in terms of the authors' classification. Table 5 gives the maximum, minimum, and average values of the residual stresses reported by the authors as well as those found in the 18WF96 shapes. The average residual stress at the center of the flange (σ_{ro}) and at the center of the web (σ_{rw}) fall outside, but the residual stress at the flange edge (σ_{rc}) falls inside the limits suggested by the authors.

An analysis of variance was made for the residual stress in the flange edge (σ_{rc}) of the 9-ft beams to determine the variation between specimens within a beam and between beams within a heat. This analysis showed that the variation in residual stress from beams of the same heat was significant, at the 1% level, when compared to the variation within a beam.

TABLE 5.—RESIDUAL STRESSES IN WIDE-FLANGE SHAPES DUE TO COOLING[a]

Member	Flange Edge, σ_{rc}			Flange Center, σ_{ro}			Web Center, σ_{rw}		
(1)	Maximum (2)	Average (3)	Minimum (4)	Maximum (5)	Average (6)	Minimum (7)	Maximum (8)	Average (9)	Minimum (10)
Authors' Columns, $d/b \leq 1.5$	-7.7	-12.8	-18.7	+16.5	+ 4.7	-4.1	+18.2	+ 8.0	-15.5
18WF96 $d/b = 1.55$	-6.7	-10.7	-13.5	+ 0.2	- 5.6	-9.5	+15.8	+11.5	+ 6.8
Authors' Beams $d/b > 1.5$	-4.1	- 7.5	-10.8	+24.2	+15.1	+8.3	- 8.8	-21.8	-41.0

[a] All stresses are given in ksi.

An analysis of variance was made to determine the variation within a beam, between beams within a heat, and between heats (the comparison between heats is confounded by beam size) for the residual stress at the flange tips (σ_{rc}) of the 2-ft beams. The variation between beams was found significant, at the 1% level, compared to the variation within a beam.

Concluding Remarks.

1. For a strain rate of 140 μ in./in. sec, the mean ratio of dynamic yield stress to static yield stress was found to be 1.08. The source of material had no effect on this ratio. Most of the test data was found to fall within the limits suggested by the authors.

2. Highly significant variation in residual stress was found to exist between beams from the same heat as well as between heats. A limited number of tests may show little variation, but as more tests are run the variation appears greater. Because a large spread in residual stresses exists from beam to beam, the test data reported by the authors appear insufficient for a reliable estimate of a generally applicable mean.

RESEARCH ON FIRE RESISTANCE OF PRESTRESSED CONCRETE[a]

Discussion by V. Paschkis

V. PASCHKIS.[8]—The author describes the expense and complication of the very elegant direct fire resistance tests that he performed and then calls for less expensive methods. The electric network analog work of which Mr. Woods speaks was pioneered at Columbia University, and, as far as the writer knows, the computer available at Columbia is the largest available in the western world (the Russians have published the availability of such a computer with 20,000 nodes; the Columbia computer has 600 nodes).[9]

As Mr. Woods explains, success or failure of a structure depends on whether the wires or cables reach a critical temperature of 800° F. A versatile computer such as the one at Columbia permits the determination of which of the several properties, heat-transfer coefficient, conductivity, specific heat, and density of the concrete, and what geometry (degree of covering of the wire) contributes most to an extension of the time to reach this critical temperature. Such a determination can be made even if the thermal properties, including the heat-transfer coefficient, are not known accurately. On the computer it is possible to vary the several variables over a wide range and thus to determine which is controlling. Then, if necessary, efforts can be made to determine these few controlling parameters more accurately.

The author suggests, as an alternate method of investigation, the use of small-scale models and states that the "scaling laws" have not been developed. If the small-scale model is to be subjected to the actual fire and loading, the scaling has to include both the mechanical strength and the thermal process. The scaling regarding the thermal process is understood, but is difficult. Assuming that the model can be made of the same material, having the same thermal properties as the original system, equal temperatures will be achieved under consideration of the following simple relationship between time scale and length scale: the ratio of time to reach a given temperature at a given point in the original system to that in the model system equals the square of the ratio of the original length dimension to the length dimension in the scale model.

However, for this simple rule to apply, the heat-transfer coefficients have to be changed in such a manner that the characteristic figure m remains constant. This figure is defined as

$$m = \frac{k}{h\,L} \qquad (1)$$

---

[a] November 1960, by Hubert Woods (Proc. paper 2640).

[8] Prof., Mech. Engrg., Dir., Heat and Mass Flow Analyzer Lab., Columbia Univ., New York, N. Y.

[9] "Mathematical Machines and Their Significance for Science and the National Economy," by V. I. Loskutov, Priborostroenniye, Instrument Construction, No. 11, 1958, pp. 8–12.

in which h is the heat transfer coefficient, expressed, for example, in Btu/ft^2, hr, F; k represents the thermal conductivity of the concrete, expressed in Btu/ft, hr, F; and L is the length. The value of h in the scale model must be changed proportionally to the change in geometric size. This, given a certain flame temperature, is exceedingly difficult to achieve, so much so that the writer would question the probability of achieving a satisfactory scale model approach, if the value h is important.

Again, to determine whether h is important, the analog computation, as indicated previously, would be inexpensive and helpful.

PRINCIPLE OF VIRTUAL WORK IN STRUCTURAL ANALYSIS[a]

Discussion by Morris Ojalvo and F. T. Mavis

MORRIS OJALVO,[12] M. ASCE.—A thought provoking and useful extension of the virtual-work theorem has been presented. One natural consequence of the article is to wonder whether the proofs can somehow be extended to cover the general case of a three-dimensional body for the purpose of achieving a better understanding of the principles on which the generalized virtual-work method depends. An attempt at a more general proof together with some physical interpretations of the virtual work theorem follows. The proof essentially follows along the lines indicated by J. B. Wilbur and C. H. Norris,[2] M. ASCE but does not introduce the concept of internal or external work.

Consider the three dimensional body of Fig. 12(a) with external forces in equilibrium and an internal system of stresses that everywhere satisfies the equations of statics. As shown in Fig. 12(b), one can consider the body divided into any number of smaller portions, each one of which is in equilibrium with the external forces acting on its original boundries and internal tractions acting on the surfaces created by the subdivision. For any traction p acting on area dA of a surface created by the subdivision, an equal but opposite traction exists on the area dA of the newly created surface that was formerly contiguous with the surface of the first particle. The two tractions p may be considered as equal but opposite vectors.

Next consider a continuous vector field $V = V(x,y,z)$ and the integral over the entire surface of a particle:

$$\iint_{\text{particle}} p \, V \, dA$$

The integration is taken over the original and newly created surfaces of the particle. The vector p is used to denote tractions on the original as well as the newly created surfaces.

By performing the integration over the entire surface of each particle and summing up, one obtains:

$$\sum_{\text{particles}} \iint p \, V \, dA$$

[a] November 1960, by Frank L. DiMaggio (Proc. paper 2643).

[12] Assoc. Prof., Dept. of Civ. Engrg., Ohio State Univ., Columbus, Ohio.

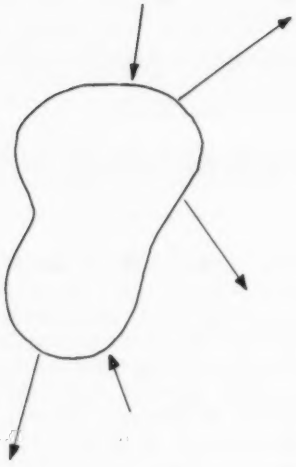

(a)

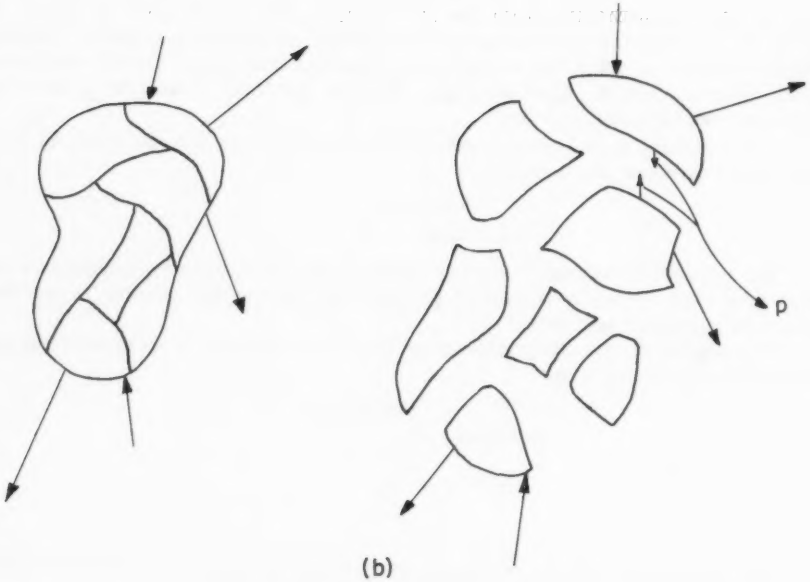

(b)

FIG. 12

The summation of the foregoing integrals vanishes for all terms involving newly created surfaces because the internal tractions p are a system of equal but opposite vectors. This means that:

$$\sum_{\text{particles}} \iint p\, V\, dA = \iint_{\substack{\text{original}\\ \text{body}}} p\, V\, dA \quad \ldots\ldots\ldots\ldots\ldots\ldots \quad (66)$$

Eq. 66 is a counterpart to Eq. 2 and expresses the theorem of virtual work.

When the vector function V is discontinuous, it is necessary to consider that the original boundary of the body includes the surfaces over which V is discontinuous. Thus, the internal tractions p at the discontinuous surfaces are treated as a set of equal but opposite external tractions and Eq. 66 is interpreted as before. When Eq. 66 is applied to a particular body the subdivisions may be taken in any manner that is convenient.

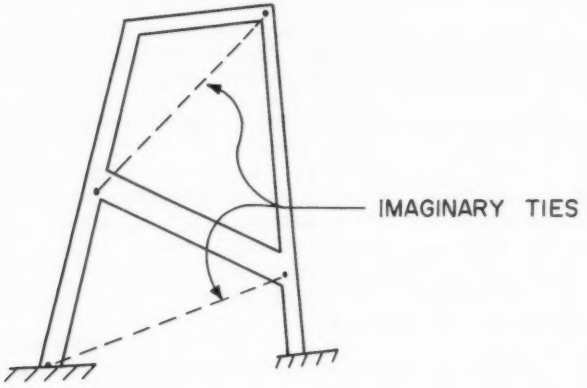

FIG. 13

The preceding proof is dependent on that principle of statics that states that for every traction one surface exerts on a second surface, the second exerts an equal but opposite traction on the first. It also requires that the virtual function be a vector function such as a displacement, velocity, or acceleration function. In all of the examples included in Mr. DiMaggio's article this latter requirement was met.

When V is a displacement vector, both sides of Eq. 66 have the units of work. When V is a velocity vector the theorem states that the time rate of the internal work is equal to the time rate of the external work.

The author contends that for frames with inclined members, the virtual-work theorem is the most efficient means of deriving equilibrium equations for use in the slope-deflection method and in the application of the lower-bound theorem of plastic analysis. Whereas this may be true for some, the writer believes that, in general, it depends on the individual's familiarity with setting up statical equations and with his familiarity with kinematic principles. The chief difficulty with the statical approach is that sometimes one ends up with

statical equations that are identities. The same kind of difficulty may exist when a kinematic approach is used because, in complicated instances, the independent mechanisms may not be apparent. To circumvent these difficulties, the writer has resorted to a method using an imaginary system of ties[13] that he has found less troublesome because it relates the kinematic problem to the problem of the stability of pin connected statically determinate trusses. For example, in Fig. 13 the equations of equilibrium other than the joint equations are those that would be used to solve for the zero stress in the imaginary ties. This device, it seems, leans to both the kinematic and the statical approach.

F. T. MAVIS,[14] F. ASCE.—So much has been written about virtual work by so many persons that "the needle" that inoculated some engineers in the mid-1920's has been lost in "the haystack" of papers on that subject. Few engineers will disagree with the author's opening sentence that

> "Although it is true that the principle of virtual work is discussed and applied in almost any modern textbook on structural analysis, even the best derivations are, probably for reasons of expediency, too restrictive to bring out the generality of this powerful idea."

Yet it would be unfortunate indeed if engineers and scientists did not share with one another in writing their rediscoveries, for example, new applications of laws that were codified by Isaac Newton three hundred years ago. But it is often overlooked that the "laws" associated with Newton's name were applied and fairly well understood by Galileo (who died the year Newton was born), and that Galileo may well have been stimulated in his independent thinking by his contemporaries and their antecedents. The point of this flash back to history is to state the premise that a stimulating restatement (as Newton's was) sometimes merits greater attention than many discoveries.

The elusive needle in the haystack of papers on virtual work, that, incidentally, is not cited by Mr. DiMaggio, is the first major publication by Hardy Cross under the appropriate title "Virtual Work: A Restatement."[15]

Cross acknowledged that most of the theorems developed in his restatement were not new nor was he "especially concerned with their lack of novelty." If his paper served

> "a useful purpose in bringing into logical sequence a group of geometrical principles which are essential to the study of statically indeterminate structures . . . the omission of references to the work of many who have helped to develop or illuminate the principle of virtual work, may be pardoned."[16]

It was characteristic of Cross to write, rewrite, and condense his thoughts into polished pellets that were stimulating but not easily digested. (His achievement in writing was purposeful and deliberate; it should be remembered that he had taught English and mathematics before he taught engineering.) Cross' restatement of virtual work has indeed a needle-like sharpness that is evident in the following quotation:[17]

---

[13] "Internal Ties in Slope Deflection and Moment Distribution," by Morris Ojalvo, Journal, ASCE, Vol. 82, No. 6, November, 1956.

[14] Dean, College of Engrg., Univ. of Maryland, College Park, Md.

[15] "Virtual Work: A Restatement," by Hardy Cross, Transactions, ASCE, Volume 90, 1927, pp. 610-618.

[16] Ibid., p. 610.

[17] Ibid., p. 612.

"The general principle deduced, therefore, may be stated, as follows: To find with reference to any line of the distorted structure and with reference to any point on that line the displacement produced at any other point by given internal distortions, consider a unit resistance to such displacement applied externally at the given point, the structure being held stable by reactions fixing the point and the line of reference. Find the internal resistances produced by this imaginary external resistance. The sum of the products of the internal distortions multiplied by the imaginary internal resistances is the desired displacement.

"The internal distortions may be due to any condition of stress and the strains may be either elastic or plastic, or they may be due to temperature or inaccurate workmanship. The external movement may be either of rotation or of translation. Rotation may be measured with reference to any line in the deflected structure. Translation may be measured in any direction with reference to any given line in the deflected structure and any given point on that line."

Then Cross gives capsulated examples under the following headings in a mere five printed pages: Virtual work applied to trusses, virtual work applied to beams, the reciprocal theorem, Greene's theorems derived directly by virtual work, Mohr's theorems, angle changes in trusses, slope deflection, and moment weights.

To apply the principles of virtual work as restated there are three steps that are wholly independent excepting that they are applied to the same "structure." These steps are as follows:

1. Tabulate systematically the (small) internal distortions in the structure. Whether these internal distortions are linear or angular and what may "cause" them is immaterial. They are merely "real internal distortions."

2. Make the "structure" statically determinate and stable with respect to a virtual load (force or couple), that Cross calls the virtual external resistance to displacement, and fix the point and the line of reference from which external displacements are to be measured, by virtual reactions. Tabulate compatibly with the internal distortions in step 1 the corresponding virtual stresses or moments. (Cross called these "virtual internal resistances.")

3. Compute the signed product (scalar product) for each pair of compatible elements in the tabulation and find the algebraic sum of these products. That sum is the external displacement with respect to the point and line of reference, in step 2, that is compatible with the given internal distortions, in step 1; and the external displacement is in the direction of the virtual load (force or couple) in step 2.

Three sentences from Cross' conclusions will show that, in his "restatement" published in 1927, there was a forshadowing of other developments in structural engineering analysis in which he was later to feature so prominently:[18]

"To apply these theorems to engineering structures, it is simply necessary either to show that for given values of the moments, shears, and thrusts, the strains can be predicted, or, of exact prediction is not possible, to determine by direct computation what error results from the in exactness . . . .

[18] Ibid., p. 618.

"Because of the definiteness of moments, shears, and thrusts, strain measurements on statically determinate structures seem for this purpose more valuable and dependable than similar data derived from measurements on indeterminate structures. When it is established that, for any type of construction, these strains—or their relative values—can be definitely predicted, the whole theory of indeterminate stress analysis follows from the relations of the distortions as a matter of geometry. In order to be a real value in designing indeterminate structures, however, the load-strain relations must be those for conditions approaching failure and not merely those that exist at working stresses. An understanding of these facts will make clearer the limitations of the theory of elasticity as applied in much of the literature dealing with indeterminate structures of reinforced concrete, will make possible the application of more correct theory to such structures, and will give greater confidence in the results obtained by its use."

If this discussion departs from the usual pattern by quoting the "needle in haystack" paper by one of his distinguished teachers, the writer makes no apology. By exposing a little of this penetrating "restatement" of virtual work he hopes that the paper that helped to usher in a fresh era in structural analysis in the mid-1920's will not pass unnoticed by serious students in the 1960's.

TENTATIVE RECOMMENDATIONS FOR THE DESIGN AND CONSTRUCTION OF COMPOSITE BEAMS AND GIRDERS FOR BUILDINGS[a]

Discussion by M. W. Kaufman

M. W. KAUFMAN,[2] M. ASCE.—The publication of the recommendations is a significant step towards the acceptance and use of composite construction in buildings and of the adoption of a governing code. The committee should be commended for the effective manner in which the research and technology in this field have been digested into practical recommendations. The use of assumptions, regarding the application of loads and the safety factor for shear connectors, simplifies design without significantly effecting the economies derived from composite construction.

There is a comment about the definition of Q in section 204.2.1. It is believed that to be more generally correct or to provide less change of misinterpretation, Q should be defined as the statical moment of the transformed area that is acting on one side of the contact surface about the neutral axis of the composite section. This, then, will satisfy the case in which the bottom of the slab and the neutral axis of the composite section are located below the contact surface.

[a] December 1960, by Joint ASCE-ACI Committee on Composite Construction (Proc. paper 2692).

[2] Structural Design Engr., Black & Veatch, Cons. Engrs., Kansas City, Mo.

PROCEEDINGS PAPERS

The technical papers published in the past year are identified by number below. Technical-division sponsorship is indicated by an abbreviation at the end of each Paper Number, the symbols referring to: Air Transport (AT), City Planning (CP), Construction (CO), Engineering Mechanics (EM), Highway (HW), Hydraulics (HY), Irrigation and Drainage (IR), Pipeline (PL), Power (PO), Sanitary Engineering (SA), Soil Mechanics and Foundations (SM), Structural (ST), Surveying and Mapping (SU), and Waterways and Harbors (WW), divisions. Papers sponsored by the Department of Conditions of Practice are identified by the symbols (PP). For titles and order coupons, refer to the appropriate issue of "Civil Engineering." Beginning with Volume 82 (January 1956) papers were published in Journals of the various Technical Divisions. To locate papers in the Journals, the symbols after the paper number are followed by a numeral designating the issue of a particular Journal in which the paper appeared. For example, Paper 2703 is identified as 2703(ST1) which indicates that the paper is contained in the first issue of the Journal of the Structural Division during 1961.

VOLUME 86 (1960)

FEBRUARY: 2355(CO1), 2356(CO1), 2357(CO1), 2358(CO1), 2359(CO1), 2360(CO1), 2361(PO1), 2362(HY2), 2363(ST2), 2364(HY2), 2365(SU1), 2366(HY2), 2367(SU1), 2368(SM1), 2369(HY2), 2370(SU1), 2371(HY2), 2372(PO1), 2373(SM1), 2374(HY2), 2375(PO1), 2376(HY2), 2377(CO1)[c], 2378(SU1), 2379(SU1), 2380(SU1), 2381(HY2)[c], 2382(ST2), 2383(SU1), 2384(ST2), 2385(SU1)[c], 2386(SU1), 2387(SU1), 2388(SU1), 2389(SM1), 2390(ST2)[c], 2391(SM1)[c], 2392(PO1)[c].

MARCH: 2393(IR1), 2394(IR1), 2395(IR1), 2396(IR1), 2397(IR1), 2398(IR1), 2399(IR1), 2400(IR1), 2401(IR1), 2402(IR1), 2403(IR1), 2404(IR1), 2405(IR1), 2406(IR1), 2407(SA2), 2408(SA2), 2409(HY3), 2410(ST3), 2411 (SA2), 2412(HW1), 2413(WW1), 2414(WW1), 2415(HY3), 2416(HW1), 2417(HW3), 2418(HW1)[c], 2419(WW1)[c], 2420(WW1), 2421(WW1), 2422(WW1), 2423(WW1), 2424(SA2), 2425(SA2)[c], 2426(HY3)[c], 2427(ST3)[c].

APRIL: 2428(ST4), 2429(HY4), 2430(PO2), 2431(SM2), 2432(PO2), 2433(ST4), 2434(EM2), 2435(PO2), 2436 (ST4), 2437(ST4), 2438(HY4), 2439(EM2), 2440(EM2), 2441(ST4), 2442(SM2), 2443(HY4), 2444(ST4), 2445 (EM2), 2446(ST4), 2447(EM2), 2448(SM2), 2449(HY4), 2450(ST4), 2451(HY4), 2452(HY4), 2453(EM2), 2454 (EM2), 2455(EM2)[c], 2456(HY4)[c], 2457(PO2)[c], 2458(ST4)[c] 2459(SM2)[c].

MAY: 2460(AT1), 2461(ST5), 2462(AT1), 2463(AT1), 2464(CP1), 2465(CP1), 2466(AT1), 2467(AT1), 2468(SA3), 2469(HY5), 2470(ST5), 2471(SA3), 2472(SA3), 2473(ST5), 2474(SA3), 2475(ST5), 2476(SA3), 2477(ST5), 2478 (HY5), 2479(SA3), 2480(ST5), 2481(SA3), 2482(CO2), 2483(CO2), 2484(HY5), 2485(HY5), 2486(AT1)[c], 2487 (CP1)[c], 2488(CO2)[c], 2489(HY5)[c], 2490(SA3)[c], 2491(ST5)[c], 2492(CP1), 2493(CO2).

JUNE: 2494(IR2), 2495(IR2), 2496(ST6), 2497(EM3), 2498(EM3), 2499(EM3), 2500(EM3), 2501(SM3), 2502 (EM3), 2503(PO3), 2504(WW2), 2505(EM3), 2506(HY6), 2507(WW2), 2508(PO3), 2509(ST6), 2510(EM3), 2511 (EM3), 2512(ST6), 2513(HW2), 2514(HY6), 2515(PO3), 2516(EM3), 2517(WW2), 2518(WW2), 2519(EM3), 2520 (PO3), 2521(HY6), 2522(SM3), 2523(ST6), 2524(HY6), 2525(HY6), 2526(HY6), 2527(IR2), 2528(ST6), 2529 (HW2), 2530(IR2), 2531(HY6), 2532(EM3)[c], 2533(HW2)[c], 2534(WW2), 2535(HY6)[c], 2536(IR2)[c], 2537(PO3)[c], 2538(SM3)[c], 2539(ST6)[c], 2540(WW2)[c].

JULY: 2541(ST7), 2542(ST7), 2543(SA4), 2544(ST7), 2545(ST7), 2546(HY7), 2547(ST7), 2548(SU2), 2549(SA4), 2550(SU2), 2551(HY7), 2552(ST7), 2553(SU2), 2554(SA4), 2555(ST7), 2556(SA4), 2557(SA4), 2558(SA4), 2559(ST7), 2560(SU2)[c], 2561(SA4)[c], 2562(HY7)[c], 2563(ST7)[c].

AUGUST: 2564(SM4), 2565(EM4), 2566(ST8), 2567(EM4), 2568(PO4), 2569(PO4), 2570(HY8), 2571(EM4), 2572(EM4), 2573(EM4), 2574(SM4), 2575(EM4), 2576(EM4), 2577(HY8), 2578(EM4), 2579(PO4), 2580 (EM4), 2581(ST8), 2582(ST8), 2583(EM4)[c], 2584(PO4)[c], 2585(ST8)[c], 2586(SM4)[c], 2587(HY8)[c].

SEPTEMBER: 2588(IR3), 2589(IR3), 2590(WW3), 2591(IR3), 2592(HW3), 2593(IR3), 2594(IR3), 2595(IR3), 2596 (HW3), 2597(WW3), 2598(IR3), 2599(WW3), 2600(WW3), 2601(WW3), 2602(WW3), 2603(WW3), 2604(HW3), 2605(SA5), 2606(WW3), 2607(SA5), 2608(ST9), 2609(SA5)[c], 2610(IR3), 2611(WW3)[c], 2612(ST9)[c], 2613(IR3)[c], 2614(HW3)[c].

OCTOBER: 2615(EM5), 2616(EM5), 2617(ST10), 2618(SM5), 2619(EM5), 2620(EM5), 2621(ST10), 2622(EM5), 2623(SM5), 2624(EM5), 2625(SM5), 2626(SM5), 2627(EM5), 2628(EM5), 2629(ST10), 2630(ST10), 2631(PO5)[c], 2632(EM5)[c], 2633(ST10), 2634(ST10), 2635(ST10)[c], 2636(SM5)[c].

NOVEMBER: 2637(ST11), 2638(ST11), 2639(CO3), 2640(ST11), 2641(SA6), 2642(WW4), 2643(ST11), 2644(HY9), 2645(ST11), 2646(HY9), 2647(WW4), 2648(WW4), 2649(WW4), 2650(ST11), 2651(CO3), 2652(HY9), 2653(HY9), 2654(ST11), 2655(HY9), 2656(HY9), 2657(SA6), 2658(WW4), 2659(WW4)[c], 2660(SA6), 2661(CO3), 2662(CO3), 2663(SA6), 2664(CO3)[c], 2665(HY9)[c], 2666(SA6)[c], 2667(ST11)[c].

DECEMBER: 2668(ST12), 2669(IR4), 2670(SM6), 2671(IR4), 2672(IR4), 2673(IR4), 2674(ST12), 2675 (EM6), 2676(IR4), 2677(HW4), 2678(ST12), 2679(EM6), 2680(ST12), 2681(SM6), 2682(IR4), 2683(SM6), 2684(SM6), 2685(IR4), 2686(EM6), 2687(EM6), 2688(EM6), 2689(EM6), 2690(EM6), 2691(EM6)[c], 2692 (ST12), 2693(ST12), 2694(HW4)[c], 2695(IR4)[c], 2696(SM6)[c], 2697(ST12)[c].

VOLUME 87 (1961)

JANUARY: 2698(PP1), 2699(PP1), 2700(HY1), 2701(SA1), 2702(SU1), 2703(ST1), 2704(ST1), 2705(SU1), 2706 (HY1), 2707(HY1), 2708(HY1), 2709(PO1), 2710(HY1), 2711(HY1), 2712(ST1), 2713(HY1), 2714(PO1), 2715 (ST1), 2716(HY1), 2717(SA1), 2718(SA1), 2719(SU1)[c], 2720(SA1)[c], 2721(ST1), 2722(PP1)[c], 2733(PO1)[c], 2724 (HY1)[c], 2725(ST1)[c].

FEBRUARY: 2726(WW1), 2727(EM1), 2728(EM1), 2729(WW1), 2730(WW1), 2731(EM1), 2732(SM1), 2733(WW1), 2734(SM1), 2735(EM1), 2736(EM1), 2737(PL1), 2738(PL1), 2739(PL1), 2740(PL1), 2741(EM1), 2742(ST2), 2743(EM1), 2744(WW1), 2745(WW1), 2746(SM1), 2747(WW1), 2748(EM1), 2749(WW1), 2750(WW1)[c], 2751 (EM1)[c], 2752(SM1)[c], 2753(PL1)[c], 2754(ST2)[c], 2755(PL1).

c. Discussion of several papers, grouped by divisions.

AMERICAN SOCIETY OF CIVIL ENGINEERS

OFFICERS FOR 1961

PRESIDENT

GLENN W. HOLCOMB

VICE-PRESIDENTS

Term expires October 1961:
CHARLES B. MOLINEAUX
LAWRENCE A. ELSENER

Term expires October 1962:
DONALD H. MATTERN
WILLIAM J. HEDLEY

DIRECTORS

Term expires October 1961:
THOMAS J. FRATAR
EARL F. O'BRIEN
DANIEL B. VENTRES
CHARLES W. BRITZIUS
WAYNE G. O'HARRA
FRED H. RHODES, JR.
N. T. VEATCH

Term expires October 1962:
ELMER K. TIMBY
SAMUEL S. BAXTER
THOMAS M. NILES
TRENT R. DAMES
WOODROW W. BAKER
BERNHARD DORNBLATT

Term expires October 1963:
ROGER H. GILMAN
HENRY W. BUCK
EARLE T. ANDREWS
JOHN B. SCALZI
JOHN D. WATSON
HARMER E. DAVIS

PAST PRESIDENTS

Members of the Board

FRANCIS S. FRIEL
FRANK A. MARSTON

EXECUTIVE SECRETARY
WILLIAM H. WISELY

TREASURER
E. LAWRENCE CHANDLER

ASSISTANT SECRETARY
DON P. REYNOLDS

ASSISTANT TREASURER
LOUIS R. HOWSON

PROCEEDINGS OF THE SOCIETY

HAROLD T. LARSEN
Manager of Technical Publications

PAUL A. PARISI
Editor of Technical Publications

MARVIN L. SCHECHTER
Associate Editor of Technical Publications

IRVIN J. SCHWARTZ
Assistant Editor of Technical Publications

COMMITTEE ON PUBLICATIONS

THOMAS M. NILES, *Chairman*

WAYNE G. O'HARRA, *Vice-Chairman*

BERNHARD DORNBLATT
HENRY W. BUCK
JOHN D. WATSON
HARMER E. DAVIS